KAMIOKA GRAVITATIONAL WAVE TELESCOPE

JGW- T1301579-v1 | *KAGRA* | 23 March 2013

Top filter assembly procedures

Riccardo DeSalvo, Luca Malerbi, Carlo Galli, Alexander Pellicone, Maddalena DeSalvo, Paolo Radaelli, Takanori Sekiguchi, Gianni Gennaro

Introduction

This is a photo gallery documenting the production process of the KAGRA Pre-isolator top filters at Galli & Morelli, Lucca Italy.

It is intended as a complement to the document JGW-T1200804: Standard filter assembly procedures. http://gwdoc.icrr.u-tokyo.ac.jp/cgi-bin/DocDB/ShowDocument?docid=804
It contains process and assembly procedures, comments, and measurements. Because many steps are the same as in the production of the standard filters, emphasis is put on the differences with respect to what reported in JGW-T1200804.

Distribution of this document:
Public

This is an internal working note of the

KAGRA Large-scale Cryogenic Graviationai Wave Telescope Project.

http://gwcenter.icrr.u-tokyo.ac.jp/en//

Baseplate comments

It has been observed in the Top filter prototype that its baseplate warped a few mm, making the implementation of the Horizontal LVDT and actuator difficult. Because of the warping, shims of various thickness were required under the IP legs and the LVDT-Actuator blocks. Two solutions were implemented to mitigate this problem: before machining. First, we annealed the Top filter base plates at 500°C in air for a few days to relax the material internal stresses that produced the warping. Second we machined the bottom surface of the Top filter to make it more compatible with shimmed LVDT-Actuator blocks.
The figure shows the surface oxidation of the base plates during machining, after annealing and prior to surface etching. The top surface of the filter was machined only where needed for assembly.

Preparation, Cleaning and Baking

About the bottom surface machining, we tried two techniques, turning on a lathe and flat milling, obtaining similar results; the warping was reduced to less than a mm across the 1.3 m diameter plate, which is an acceptable value with redesigned LVDT-actuator blocks, eliminating shims under the Inverted Pendulum legs.
The GAS filter blade emplacements on top surface were machined after the bottom surface to guarantee best co-planarity of the blades' feet.

After machining, cleaning and etching, the base-plates were further baked 24 hours at 200°C to induce all possible warping before assembly, and for UHV cleanliness.

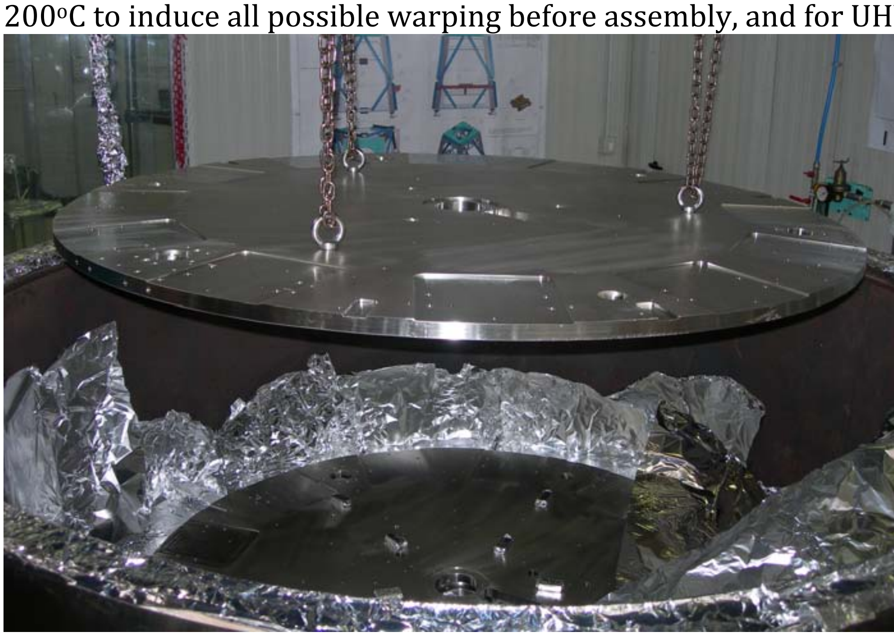

All the other components were similarly inspected, then washed and baked at 200°C for 24 hours for UHV compatibility. The blades's base blocks are shown below

One of the keystones at the center of the GAS filters:

All parts were loaded in a baking canister and protected with aluminum foil.

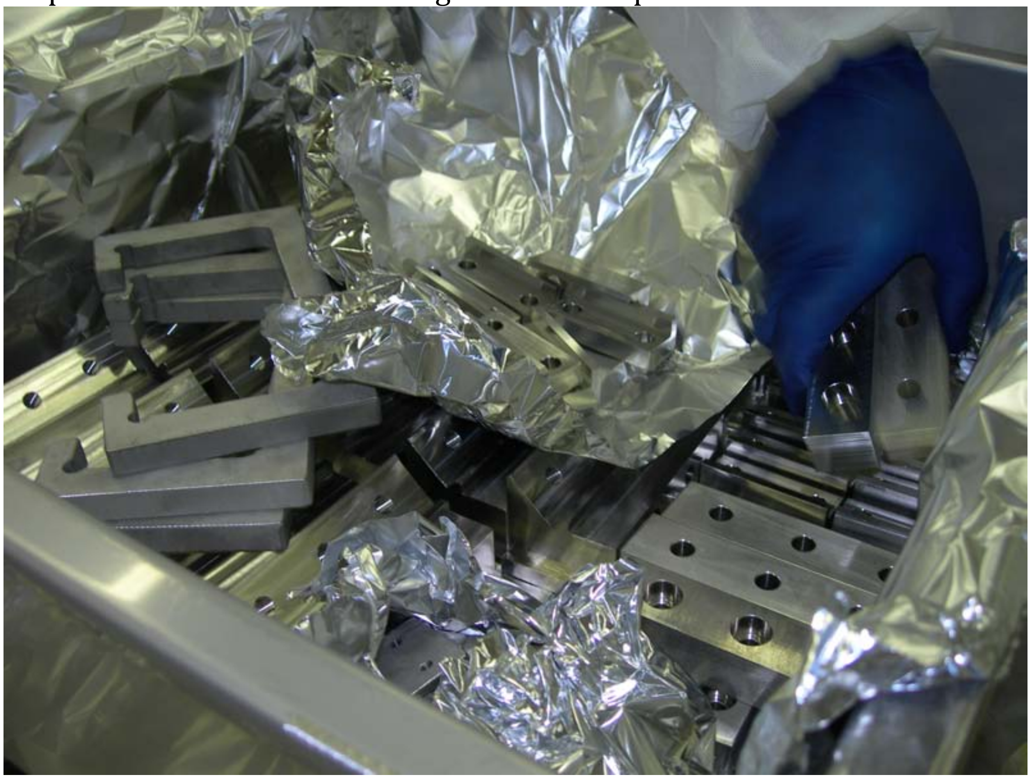

The canisters are then lowered in the oven for air bake at 200^{o}C for 24 hours.

Cantilever Blades

The blades were precision ground to a pre-selected thickness. Due to lack of raw Maraging at the time of production (Aubert-Duval delivered very late), we were forced to produce the blades from maraging sheets that were too thin. As a result, and because of an error, several rejects were produced and not all desired thicknesses could be produced immediately (as described in the blue text in the next two pages).

The thickness of all blades was checked with a Palmer micrometer and, more precisely, with an electronic scale with 1 g error over 2100 g weight. The mass is proportional to the average thickness, therefore a better indicator of the blade's strength as a spring. A mass fluctuation of only 0.1% between blades was measured.

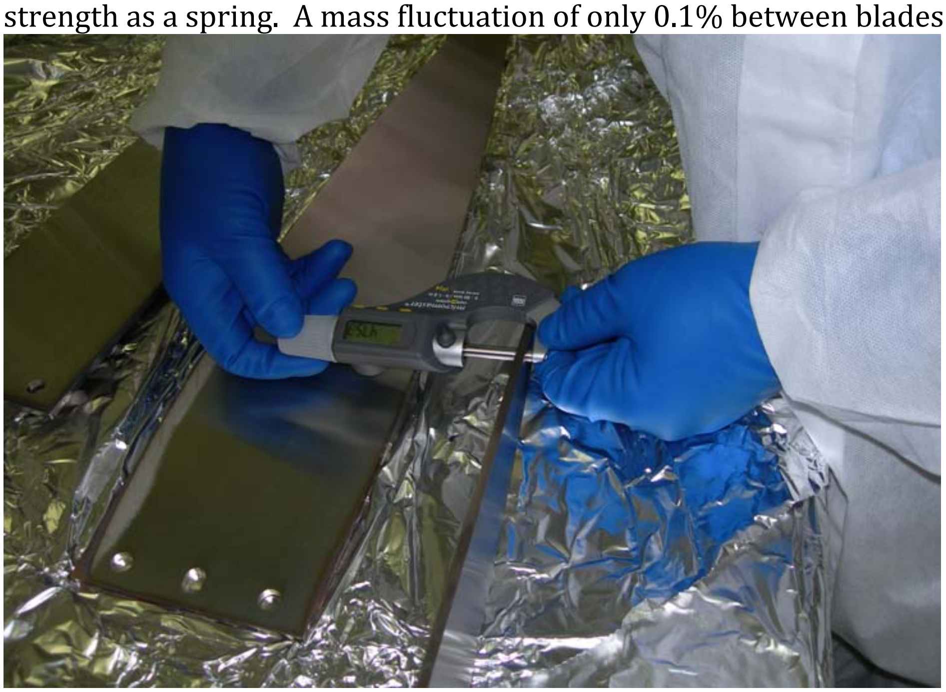

Because of lack of material at the time of production, some of the blades, to completes the filters of type A will be produced next year together with the balance of 5 Top filters.

We measured the weight and load of the blades.
Load:
255 kg for A (three blades)
274.5 kg for B1
299 kg for B2
Blade Weight:
2121.4 g for A
2173.0 g for B1
2241.7 g for B2

Nominal Blade thickness:
4.65 mm for A
4.75 mm for B1
4.9 mm for B2

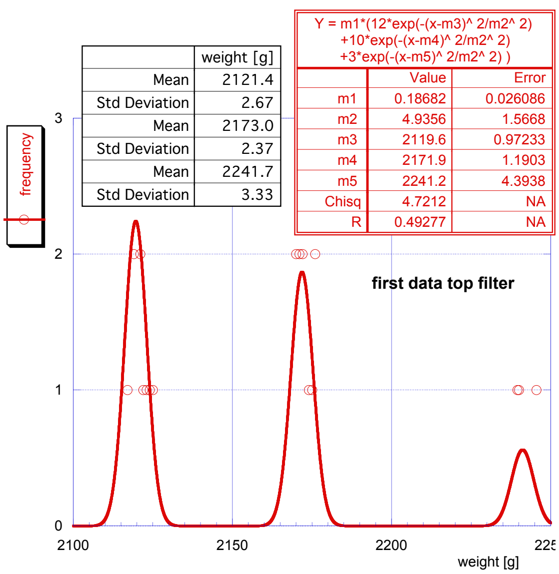

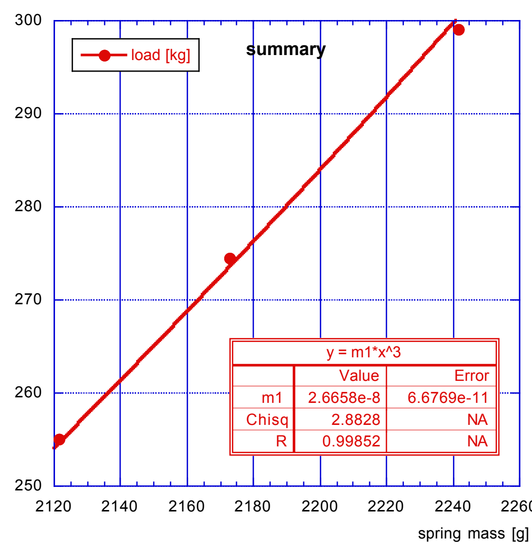

I found is a serious problem, when I compared the required load from the springs of type A, B1 and B2, and the available maraging before the delivery from Aubert Duval, I got the required load values from drawing 11000, 10000 and 00013.
My mistake was that I used in the calculations the type A top filter mass 474.4 kg instead of its required load 581.12 kg.
As a result I concluded that we had enough maraging before next delivery from Aubert Duval to build the 6 filters needed this year. This was possible at the price of making different blade thicknesses for different types of filters.

Eventually we realized that we had barely enough to build the 6 filters only if my wrong target of 474.4 kg for filter type A was assumed, and not enough for the 581.1 required load.
I discovered the mistake while calculating how much do we need to trim the blade widths, and came with a number larger than 1 as illustrated in table 1.
What to do?
For type B1 and B2, because the excess load capability is small (11 and 16 kg) we decided not modify the blades, and just add 11 or 16 kg ballast mass on filter 1.
For type A, we cannot deliver in time filters with 6 blades according to the load specs. Thicker replacement blades could be manufactured staring in February, after the delivery from A&D, but not in time for delivery by April 1st in Japan.

It was decided to mount the type A with 3 blades only, and then build a complement of three 5.1 mm thick blades together with the production run of next year. The complement of blades will be shipped pre-stressed on 6 bending tools 0921, in UHV state, and will be added in Japan to the two type-A filters in the existing clean rooms in Akeno with no additional tooling.
Note that the material that has finally arrived from Aubert Duval is 6 mm thick, therefore producing 5.1 mm thick blades is now easily possible. Their load would be 337 kg, which added to the 255 Kg of the blades in use for type A would give 592 kg load, well satisfying the required 581.12 kg load.
The final blade choice is summarized in table 2.

Table 1 Original calculation of thicknesses and load

type	load [kg]	required load [kg]	number of blades	required load per blade [kg]	measured load per blade[kg]	Width trimming required	Excess load capability [kg]
A	255.00	581.12	6.	96.853	85.000	1.1394	-71.120
B1	274.50	258.40	3.	86.133	91.500	0.94135	16.100
B2	299.00	287.85	3.	95.950	99.667	0.96271	11.150
mistaken A		474.00	6.	79.000	85.000	0.92941	

Table 2 Final calculation of thicknesses and load

type	Thickness [mm]	load [kg]	required load [kg]	number of blades	required load per blade [kg]	measured load per blade[kg]	Excess load capability [kg]
A-a	4.65	255.00	581.12	3.	85.00	85.000	
A-b	5.1	337.00	581.12	3.	112.33	tbc	9.
B1	4.75	274.50	258.40	3.	86.133	91.500	16.100
B2	4.9	299.00	287.85	3.	95.950	99.667	11.150

After selecting the blades of perfect quality, we piled them up, wrapped in aluminum foil, compressed between two flat plates in preparation for precipitation hardening of the maraging at 435ºC for 100 hours in Argon atmosphere.
The flat plates are intended to relax all internal stresses during precipitation while keeping the blades flat. As a result the residual warping of the blades after baking was measured well below 0.5 mm.

Pre-stressing the cantilever blades

Pre-stressing the blades of the top filter was much more difficult and dangerous than for the standard filters, because the top filter blades hold about 1000 N load (more than twice than the standard filters) and stretch over more than twice the distance.
A new machine to safely bend the blades was designed, using a commercial recirculating balls linear actuator as shown below.

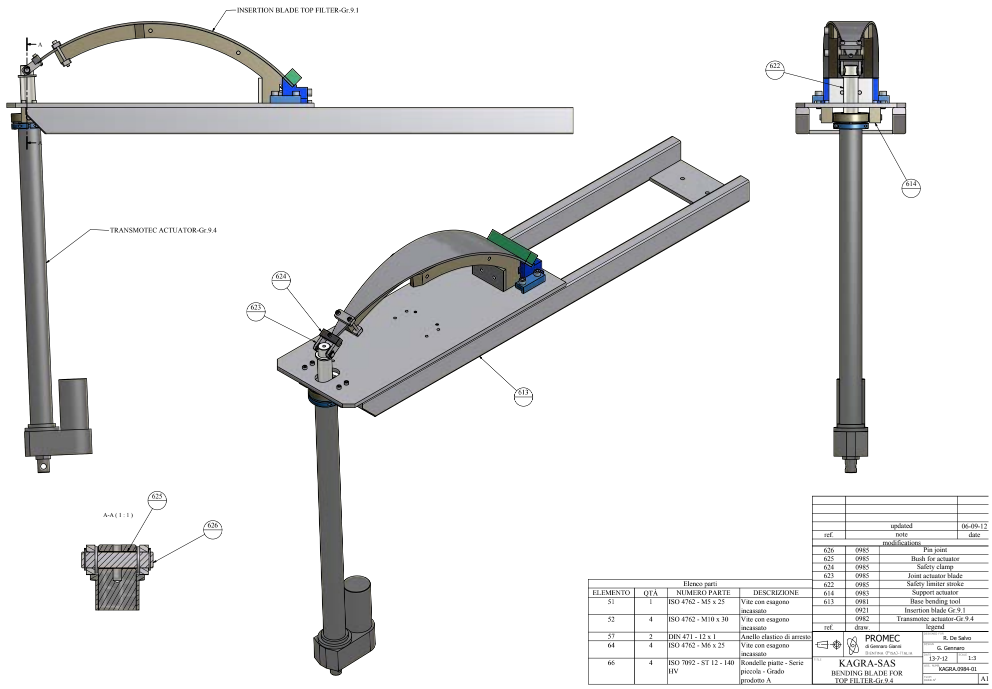

The photo shows the size of the actuator and of the blades. The drawing shows how the –pre-stress is held after the blade has been pulled, before it is mounted on the filter. Please also see the related movie in JGW-G1301580. http://gwdoc.icrr.u-tokyo.ac.jp/cgi-bin/DocDB/ShowDocument?docid=1580

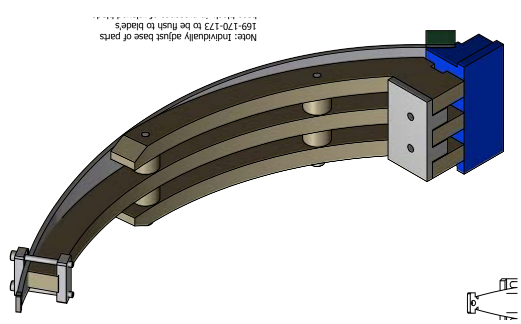

Pre-stressing sequence.
The blade's base block is bolted to to the bending tool and the three pre-stressing arches bolted to the base block

the blade mounted on the block

the actuator head is attached to the nose of the blade

The actuator head can swivel and has a slot that accepts the blade's nose. A safety cap entraps the nose in the actuator head and is held by a screw passing through the hole in the blade's nose.

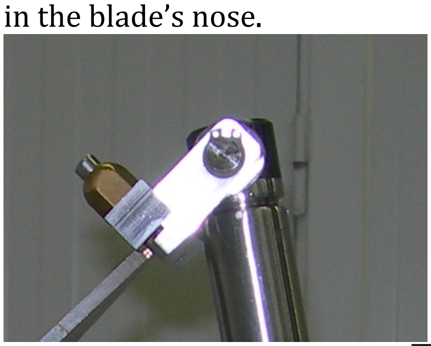

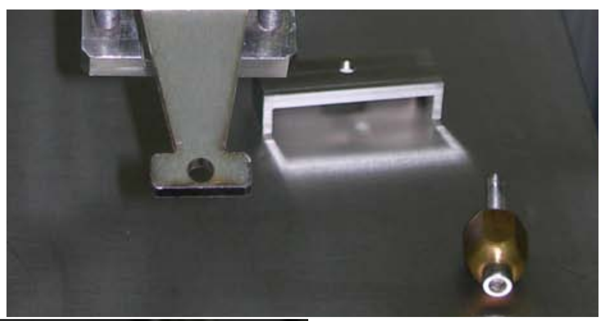

The actuator is then used to pull the blade to its required bending and stress.

until it lies on the pre-stressing arches

Then the blade is clamped to the tip of the central bending arch by means of a bolted clamp.

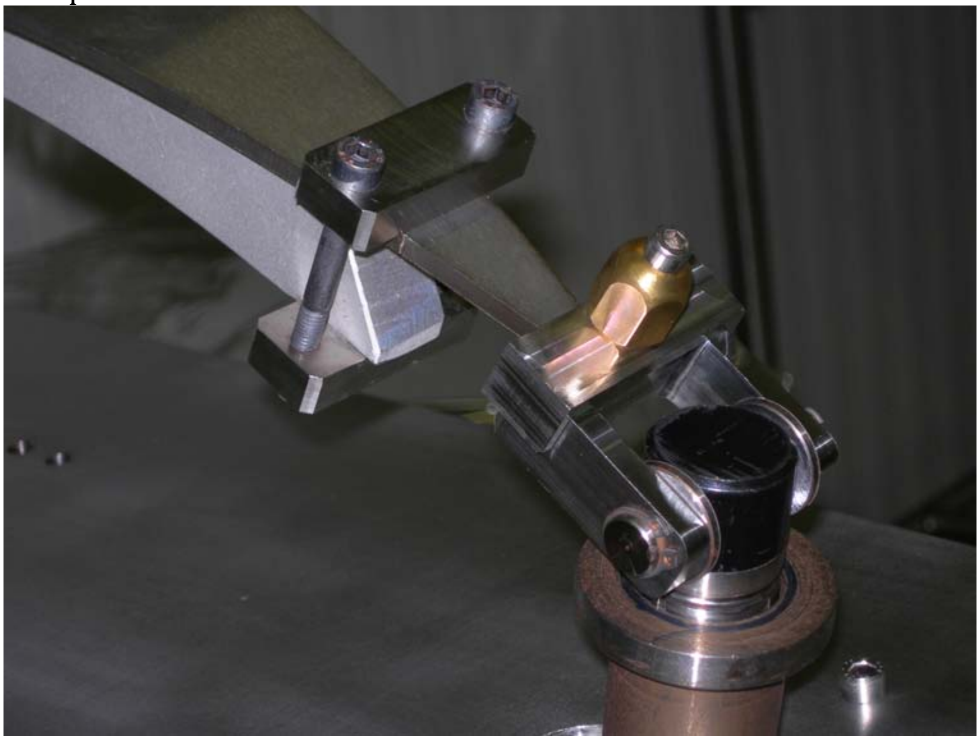

The actuator is disconnected, from the blade

the block is unbolted from the tool and the pre-stressed blade is ready for assembly in the filter.

Cantilever Blades and keystone assembly

After UHV baking, the clean room crane is used to flip the filter base plates and inspect both sides

The base plate is then lifted from the inspection bench and moved to the assembly and testing tower

The base plate is positioned on the assembly tower

The keystone holding tool is fastened below the base plate.

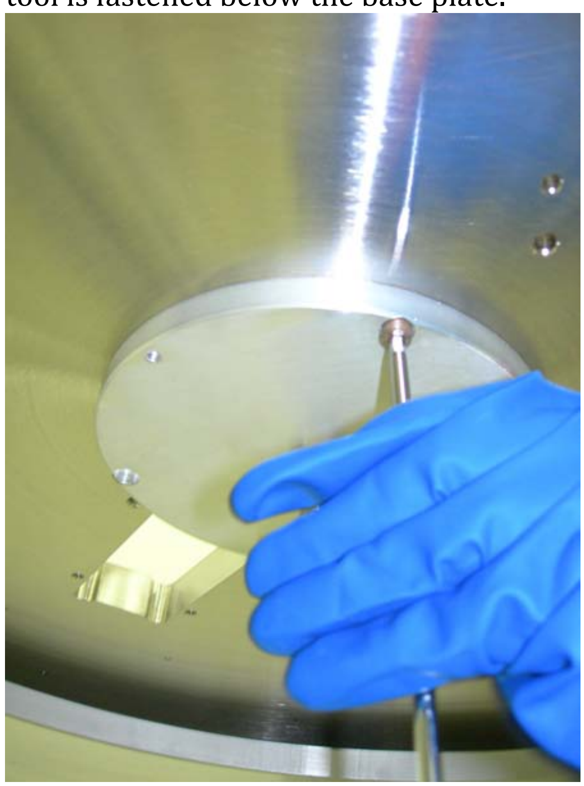

The keystone is mounted on its holding tool; the three columns holding the keystone end-stop plate are mounted as well to provide angular alignment. The two keystone magic wand attachments are oriented towards the magic wand emplacements on the base plate.

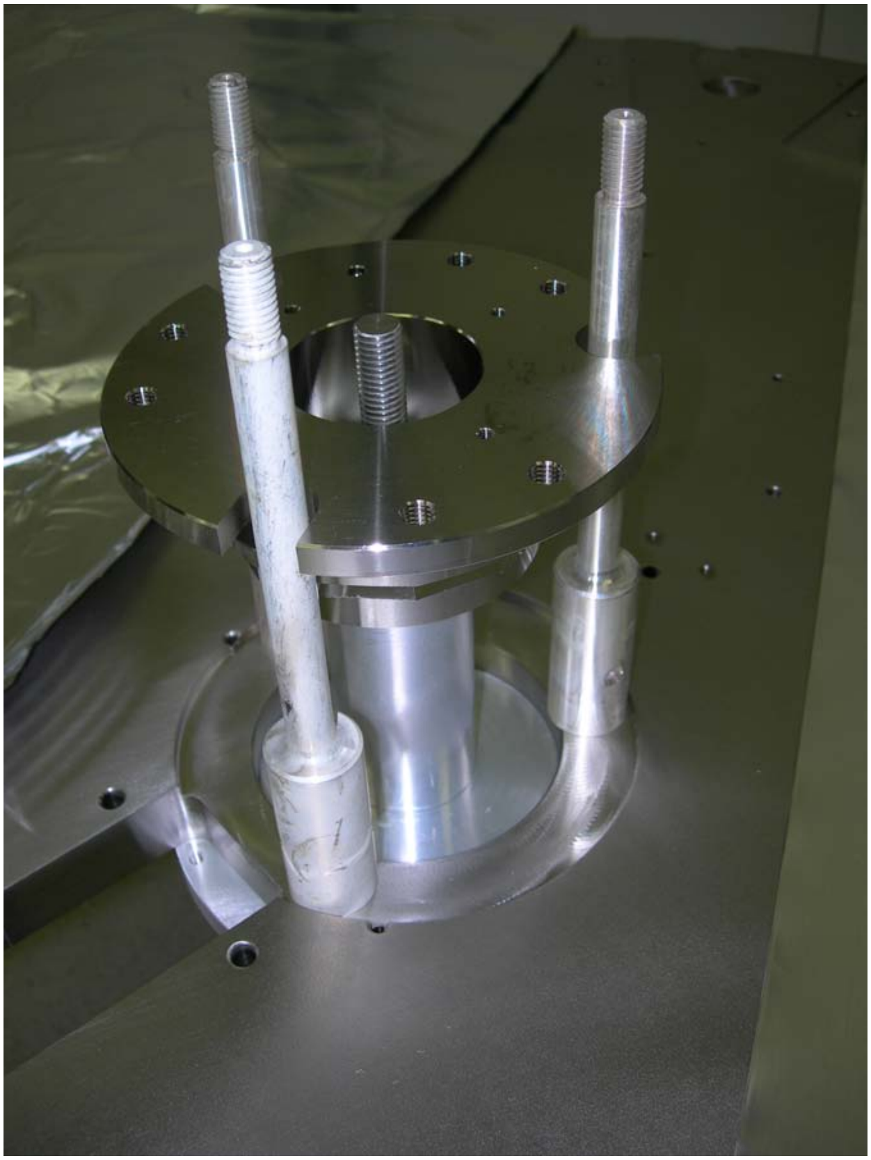

Three temporary centering spacers are inserted on the columns for precision definition of the angular positioning of the keystone during assembly of the blades. The blades are then presented to the keystone.

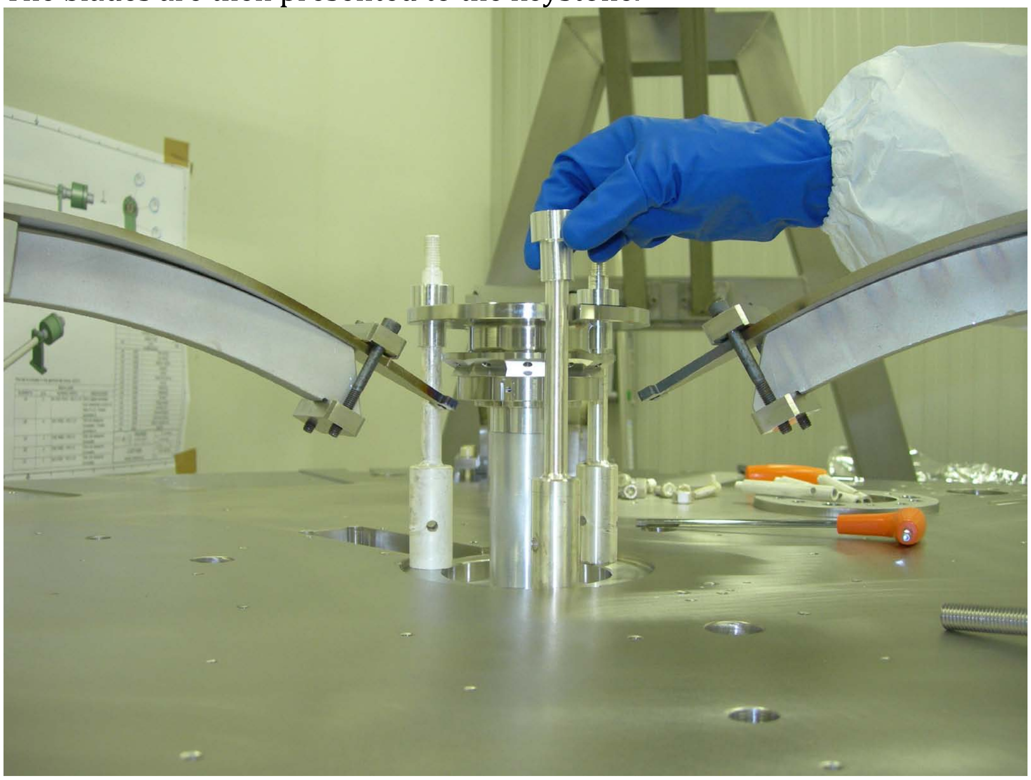

The keystone is fastened to the holder with its central threaded rod

and then locked tight.

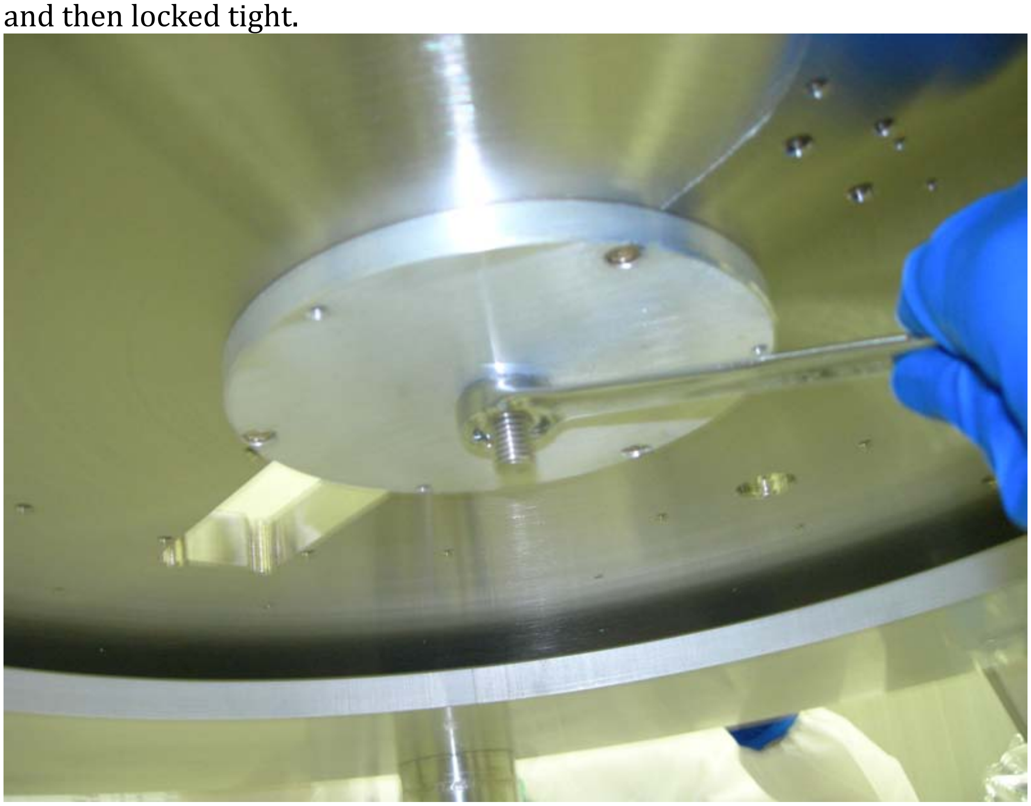

The blade's noses are screwed to the keystone while their feet are still loosely held by the feet clamps.

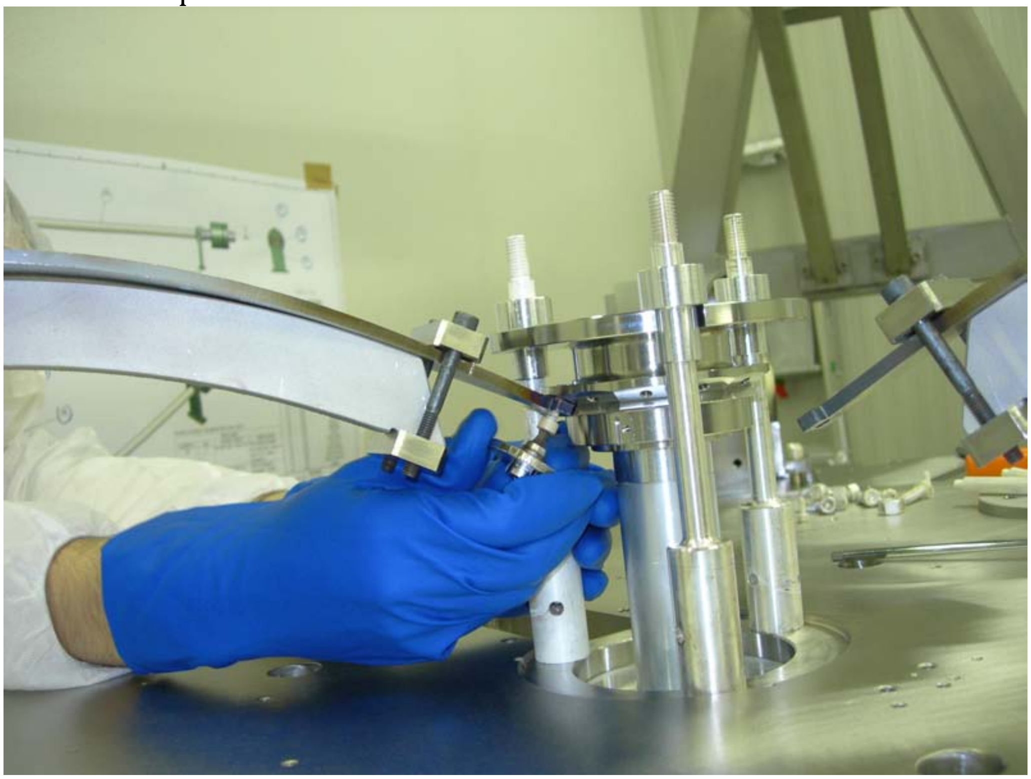

all the blade noses are tied:

Then the clamps holding the blade base blocks are tightened

To release the pre-stressed blades the holding screws are lubricated with ultrapure alcohol

The nose-holding screws are released, half a turn each going around, and around and around, until the stress is completely and symmetrically transferred to the keystone, and the nose clamps can be removed

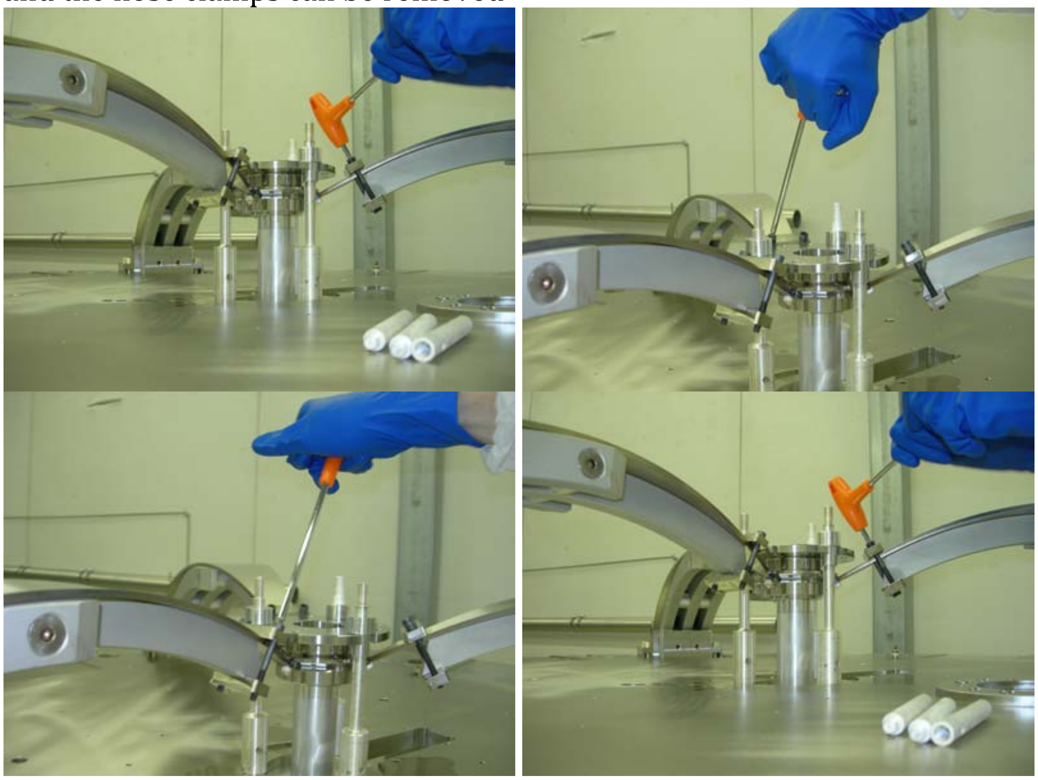

Then the pre-stressing arcs are released from the blade bases and removed.

After the blade noses are well seated, the three centering spacers are removed

and the keystone end-stop plate is mounted and locked in place, and the columns supporting the rotational mechanism's plate are added.

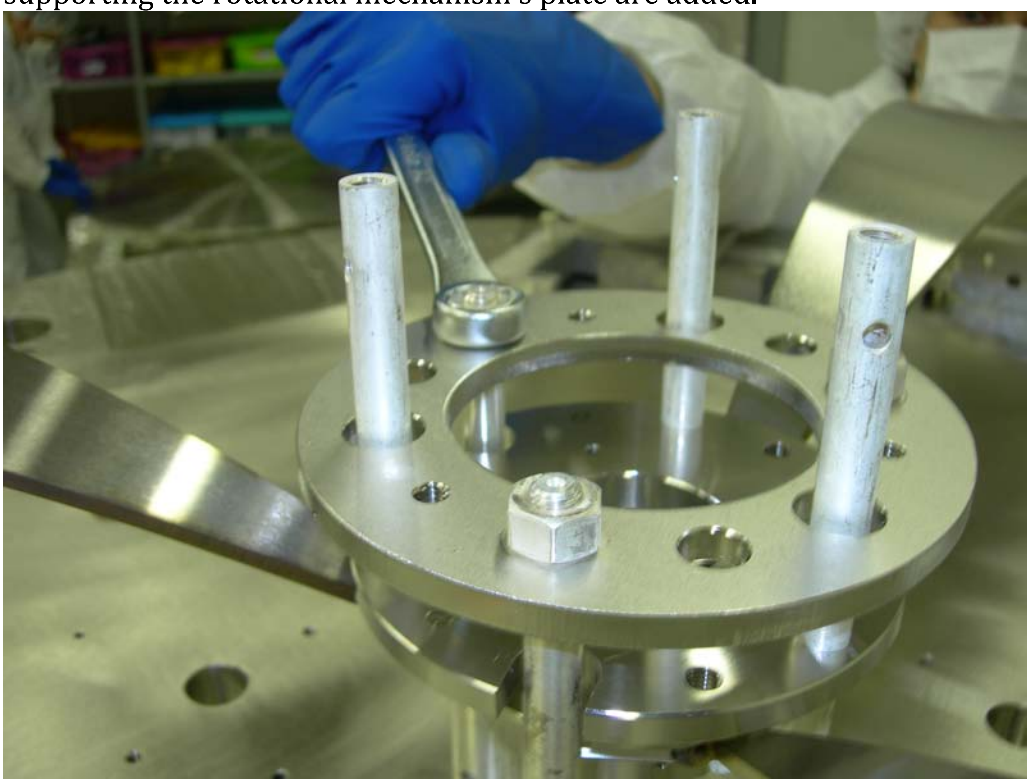

the upper and lower end-stop screw are mounted, and brought to contact in preparation for the stress transfer from the keystone assembly tool to the endstop plate.

The rotation mechanism plate is mounted on its columns and locked

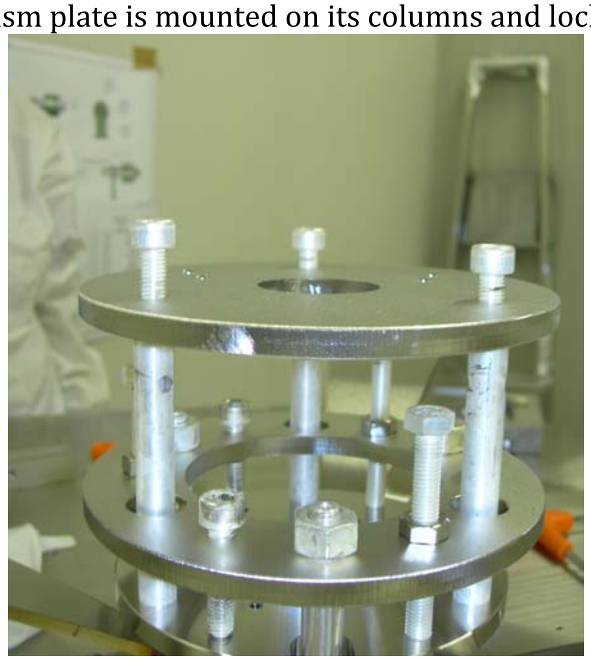

The keystone locking threaded bar is loosened and removed

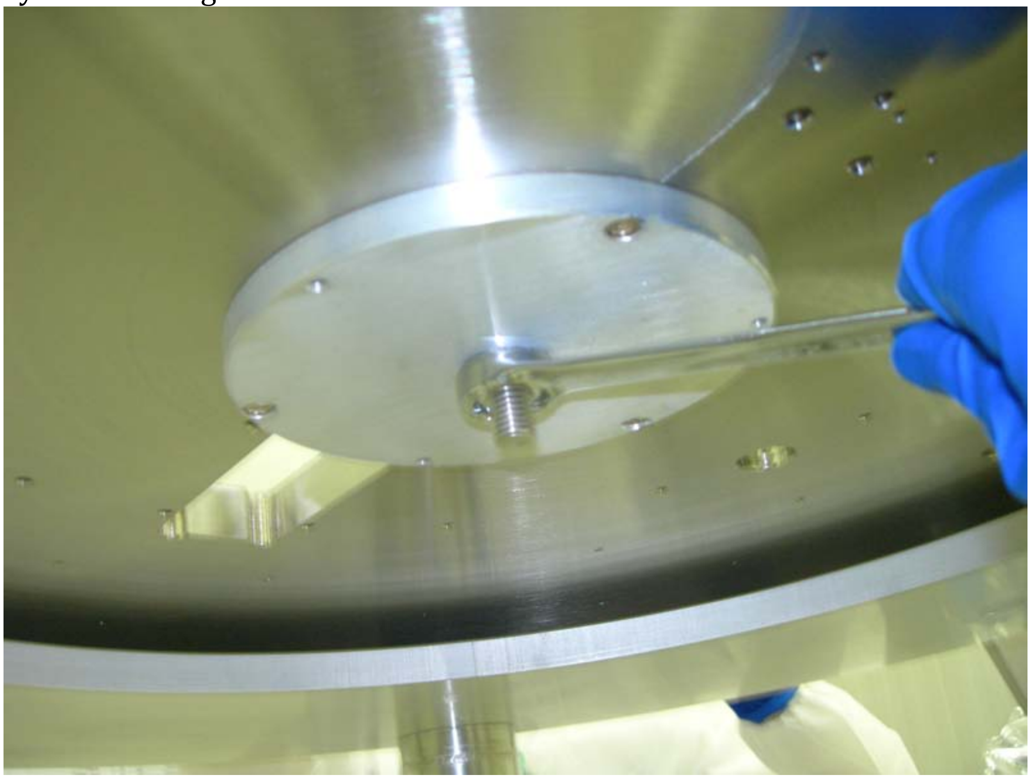

The keystone holding tool is also removed

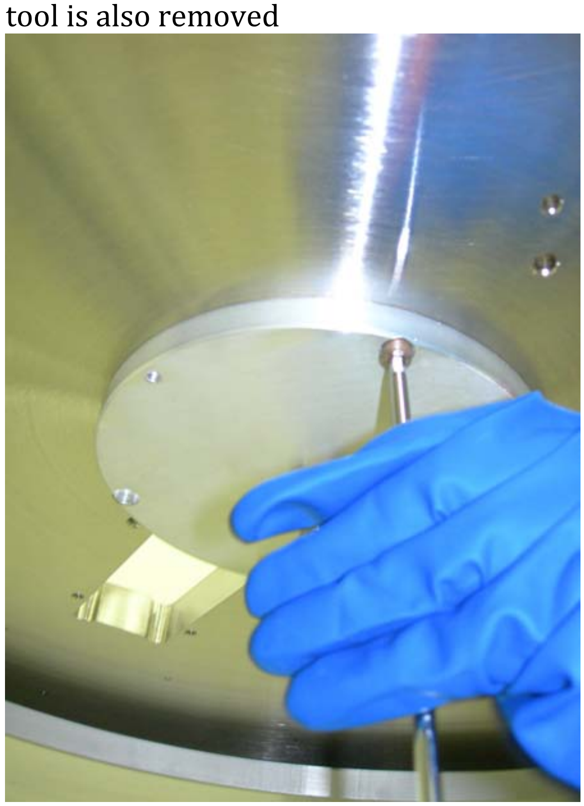

The filter is ready for tuning. The lower end-stop screws are released.

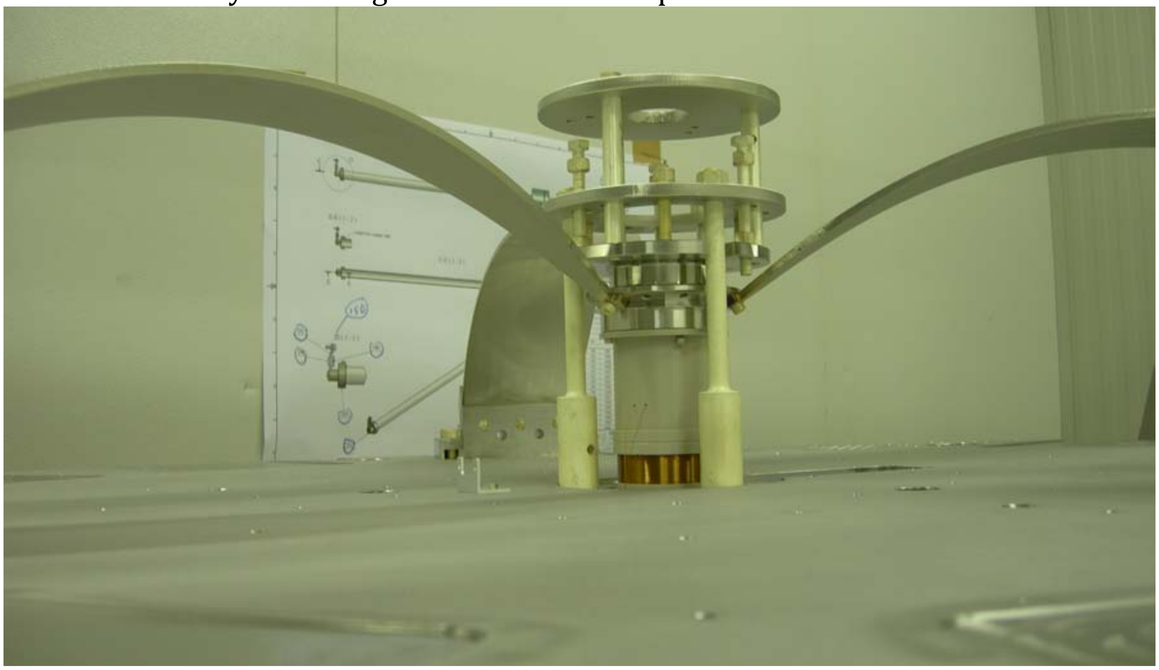

A 1 m long threaded rod is attached inside the keystone, and loaded with slotted load disks of various weights, until the filter starts floating and the upper end-stop screws can be retracted. Suitable safety stands below the disks insure against accidents.

Frequency tuning

A millimetric stick is placed on the keystone, measuring the height between the keystone and its end-stop.

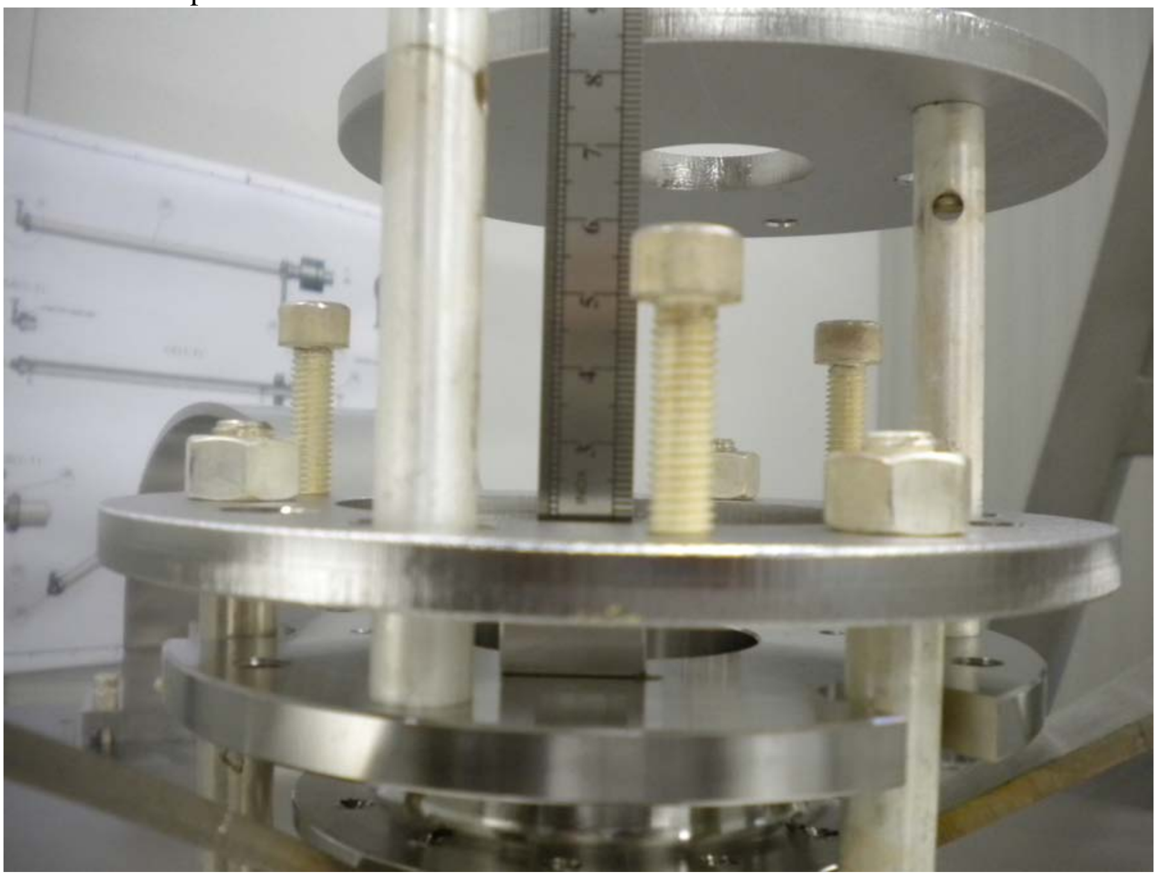

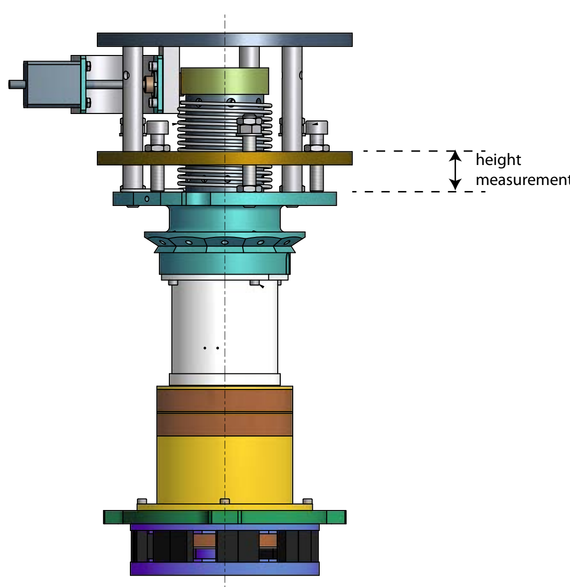

The filter oscillation period is measured with a stopwatch, typically over 10 or 20 oscillations. A smaller number of oscillations is measured at very low frequency. Mass, Frequency, height of the keystone and temperature are noted.
The mass is varied to get at different working heights, the excitation is measured and plotted versus height to find the optimal working point.

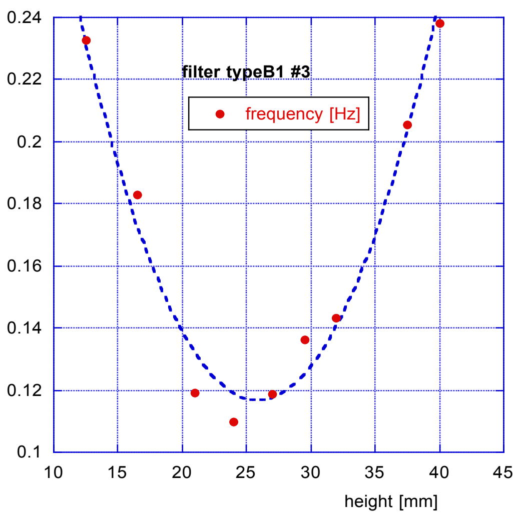

The resonant frequency of the filter is tuned by changing the radial compression of the base blocks of the three blades. For this operation
a pushing horseshoe is mounted on the clamps tieing the base blocks,
the M12 pushing screws are brought in contact with the back of the base block,
the four screws of the two clamps are released ¼ of a turn,
the pushing screws are used in ¼ turn increments to advance the base block
the four screws of the two clamps are re-tightened,
the horseshoe is removed

The radial compression is performed symmetrically and progressively on all three blades.
The radial compression is measured as illustrated below.

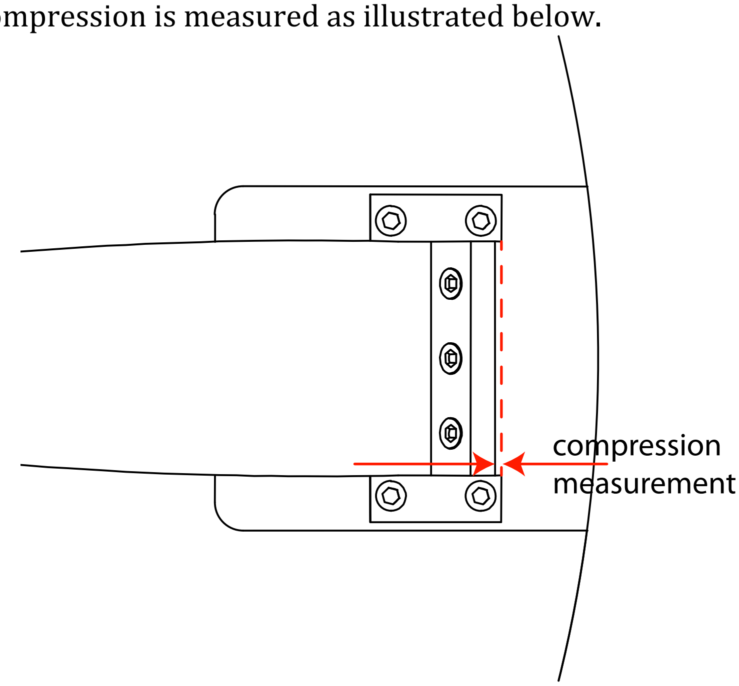

The frequency versus radial compression graph follows the expected square root law. A typical compression of 15 to 16 mm is necessary to lower the filter's resonant frequency to a suitable value (below 200 mHz).

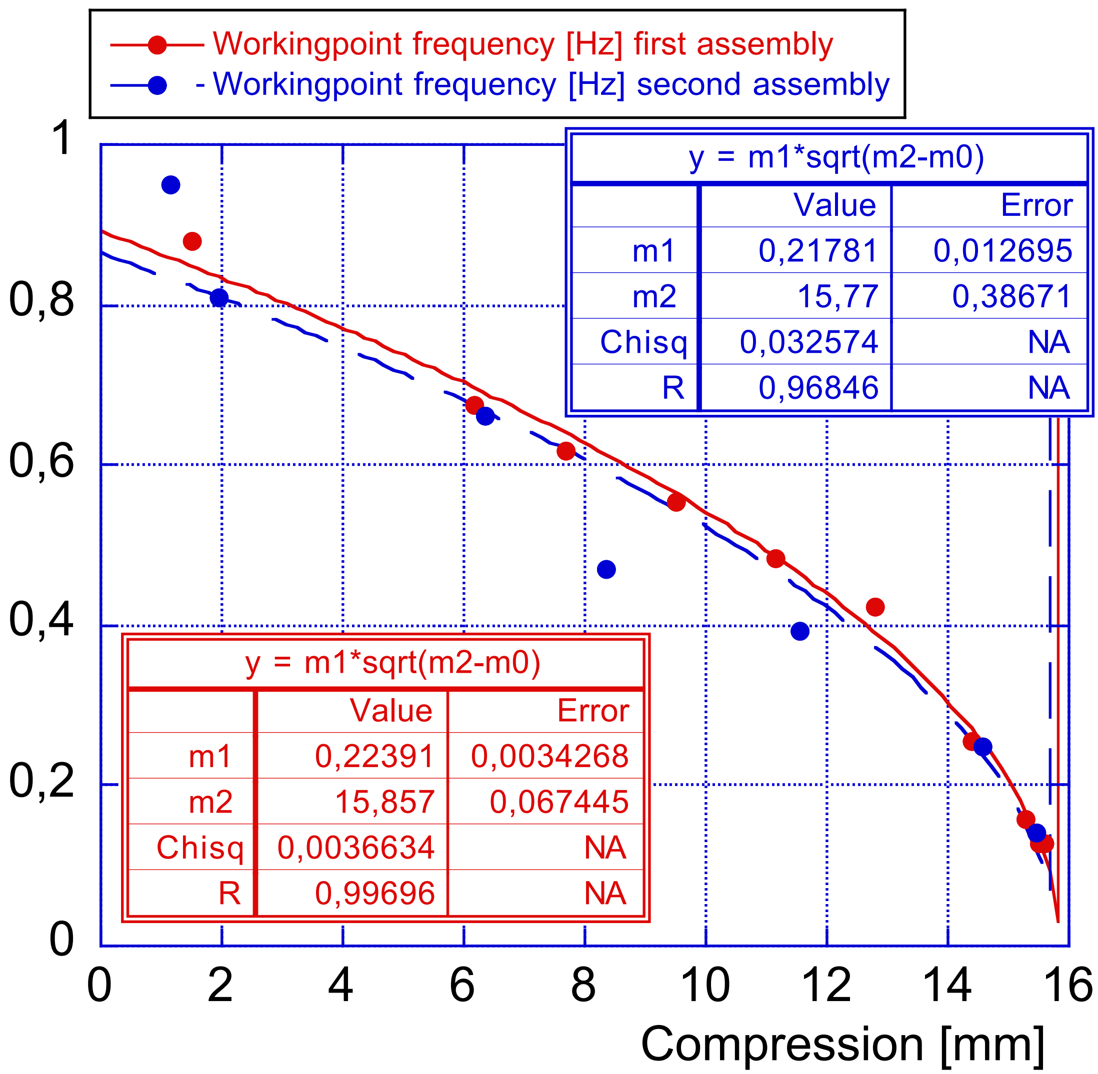

A strange behavior was documented for the optimal working point of the filter. When first tuning a filter after assembly, it was found that, instead of changing little with radial compession, the working point drifts tens of mm, and then jumps to a different position when the compression is sufficient to bring the resonant frequency near the desired level. The problem was identified with an incomplete seating of the noses of the blades in the keystone. At sufficient radial compression the noses click in place and the filter works correctly. The screws holding the noses are then re-tightened. After this, if the radial compression is released and re-increased, the working point remains stable, i.e. drifts a few mm only.

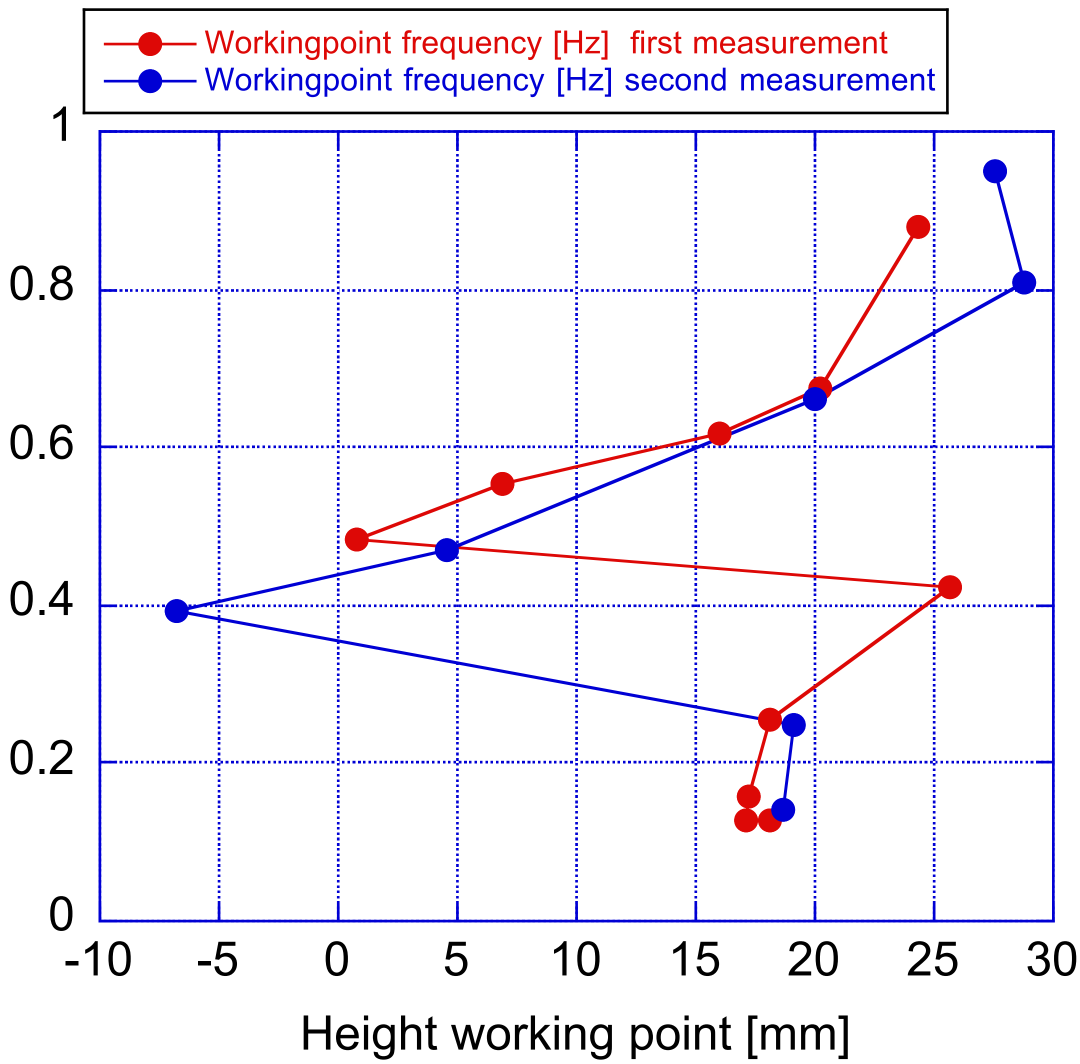

All six filters were thus tuned and characterized.

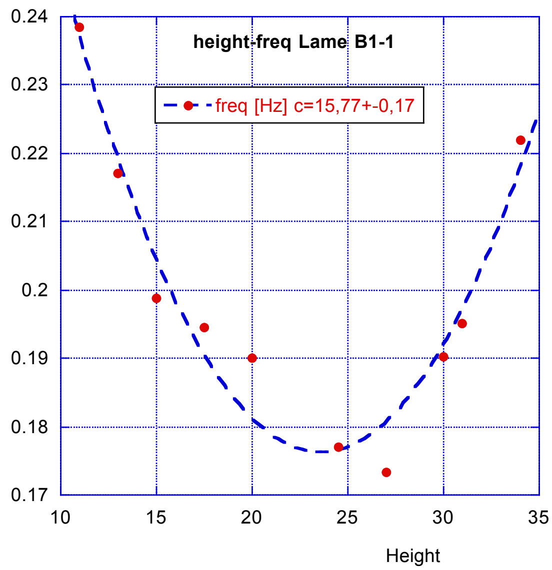

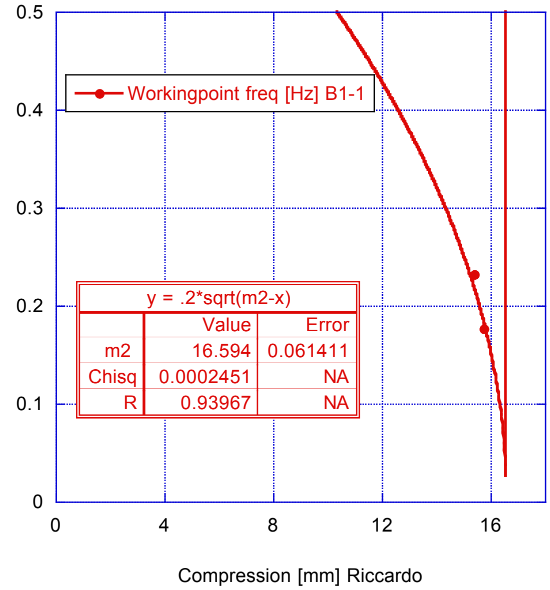

filter B1-1
working point 23.6 mm frequency 0.176 Hz
working mass 274 kg at 22.4°C
compression 15.77 ± 0.17 mm

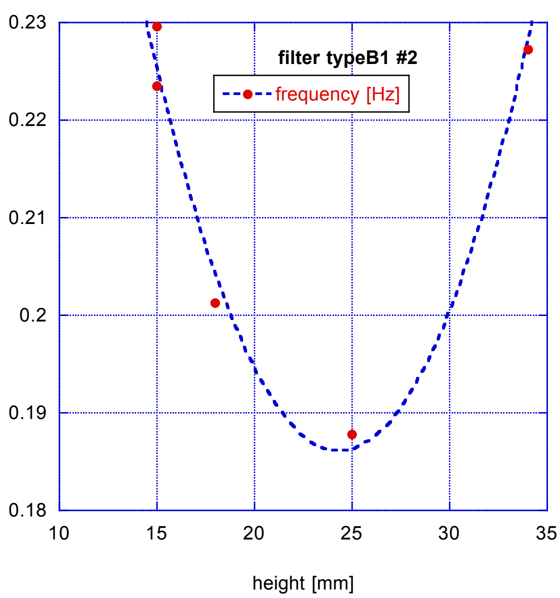

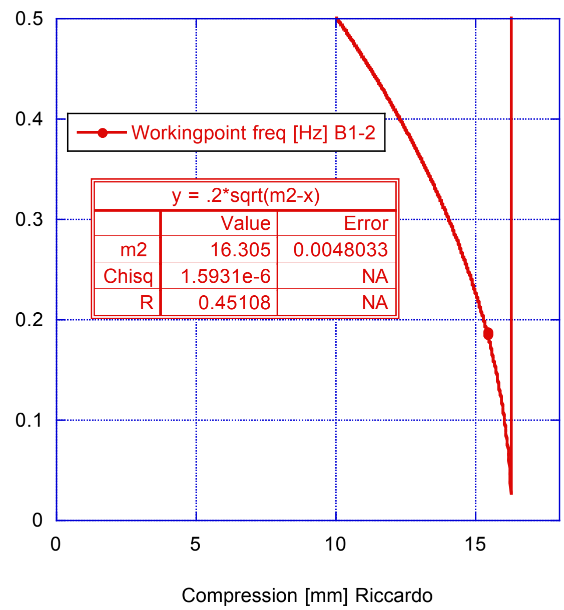

filter B1-2
working point 24.6 mm frequency 0.186 Hz
working mass 276 kg at 21°C
compression 15.44 ± 0.07 mm

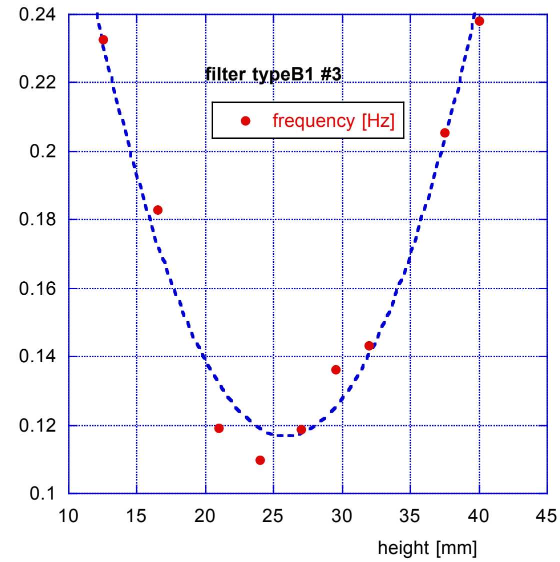

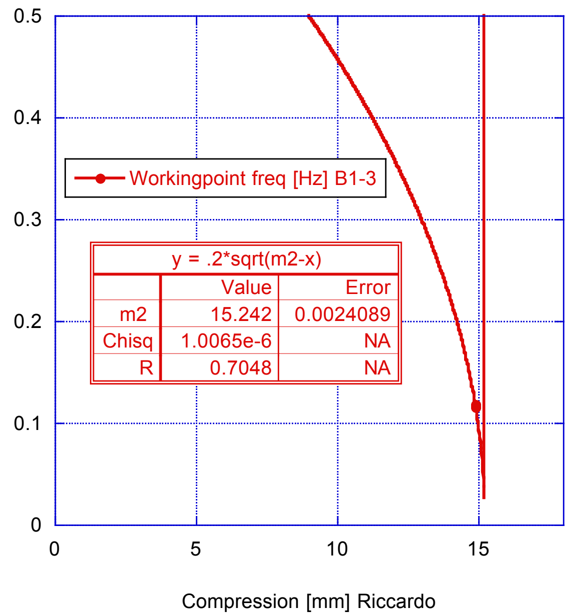

filter B1-3
working point 25.8 mm frequency 0.117 Hz
working mass 276 kg at 20°C
compression 14.9 ± 0.1 mm

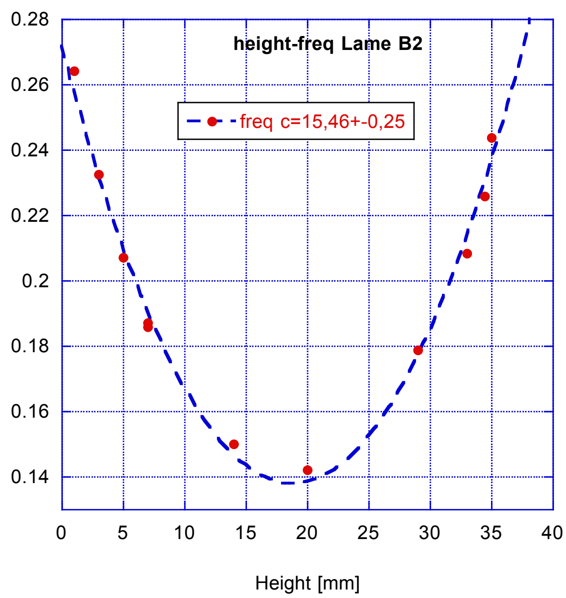

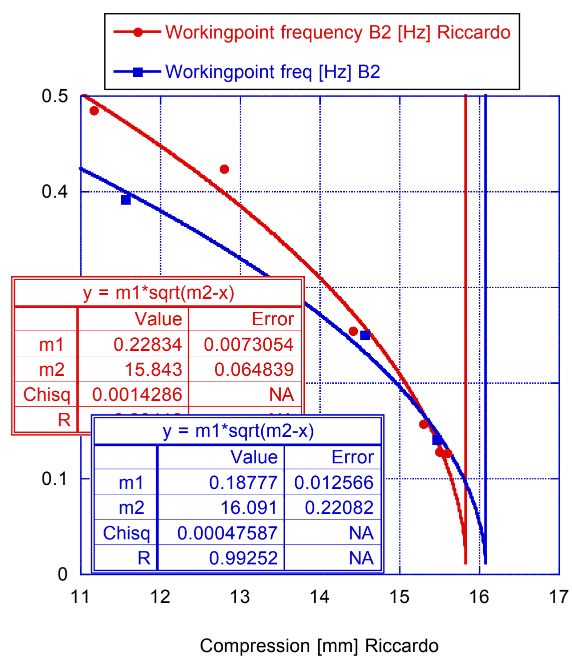

filter B2
working point 18.4 mm frequency 0.138 Hz
working mass 301 kg at 23.5°C
compression 15.46 ± 0.25 mm

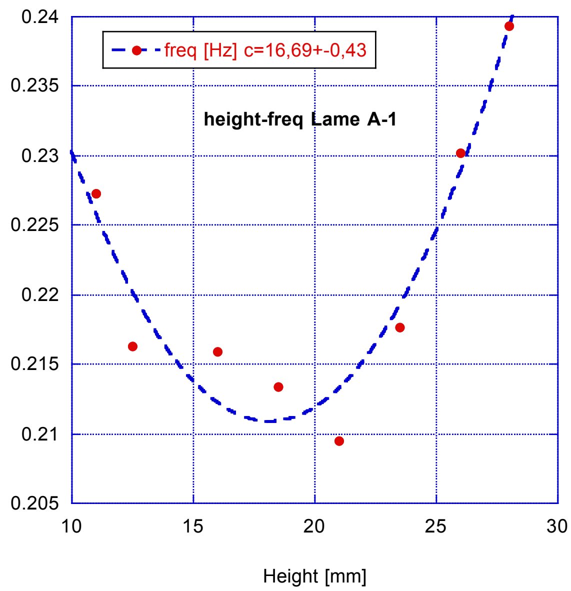

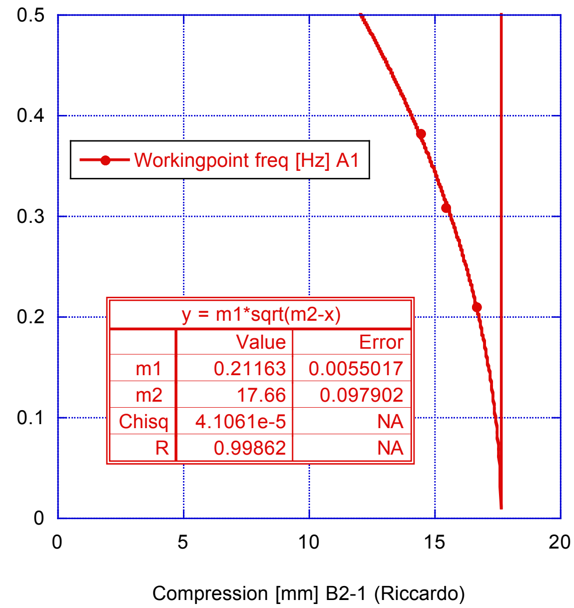

filter A1
working point 18.2 mm frequency 0.211 Hz
working mass 210 kg at 20.8°C
compression 16.7 ± 0.4 mm

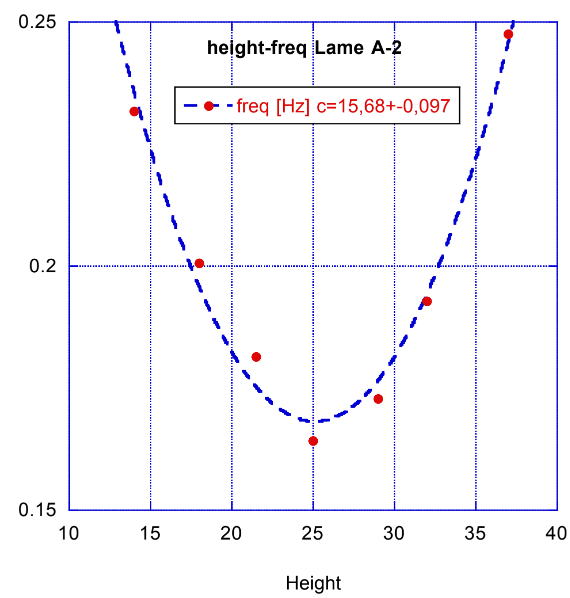

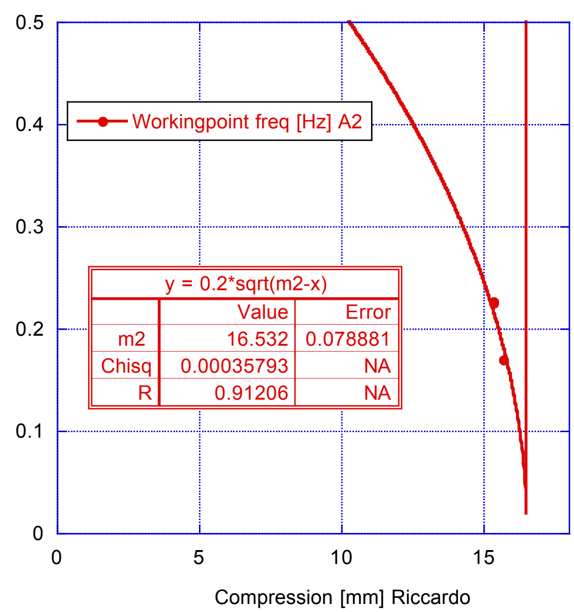

filter A2
working point 25.1 mm frequency 0.168 Hz
working mass 209 kg at 20.8°C
compression 15.68 ± 0.1 mm

LVDT and actuator Coil assembly.

The LVDT primary and actuator coil are inserted in the filter from below

A second operator holds the coil and orients the wiring towards the connector stand

The first operator screws the coil holder in place below the keystone

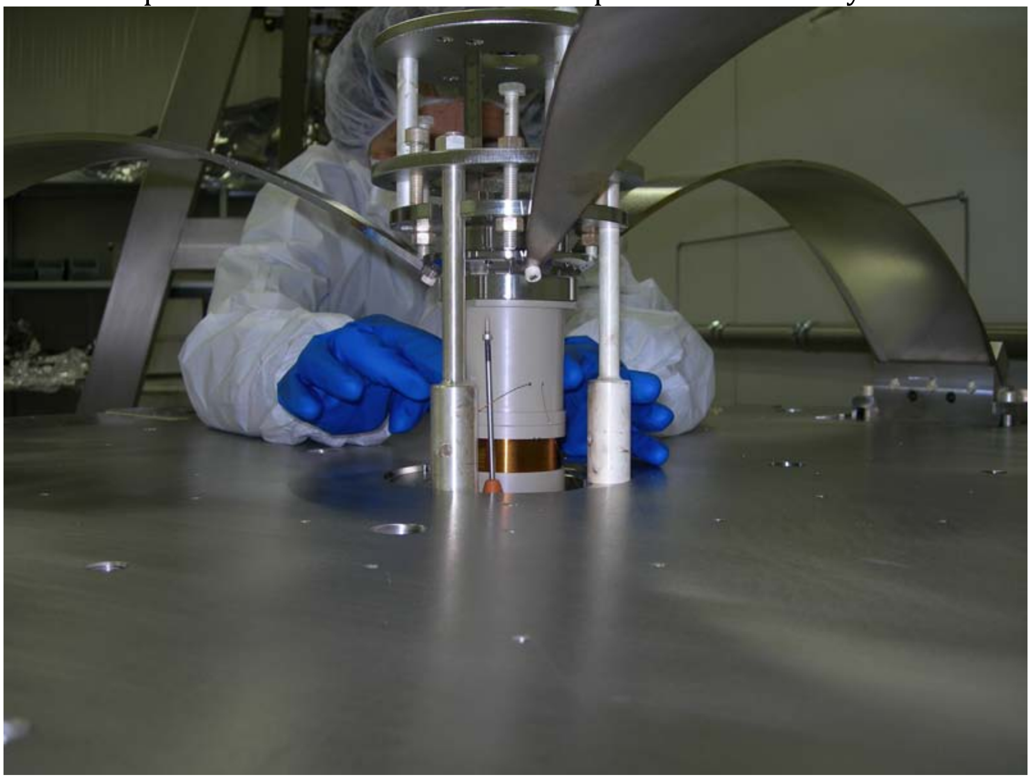

The LVDT primary and actuator wires are brought up to the top surface of the base plate.

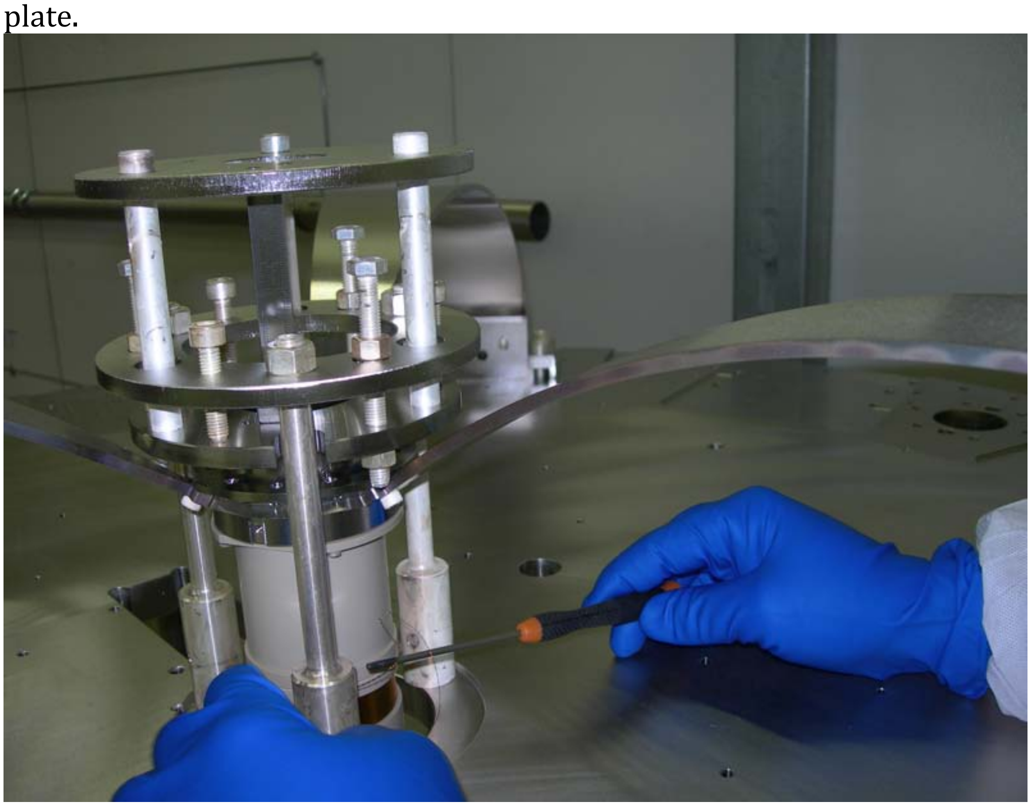

The voice coil magnets and the LVDT secondary coils are assembled in the same way of the standard filters (JGW-T1200804). The pusher screws of the LVDT secondary are pre-mounted, about 15 mm sticking through

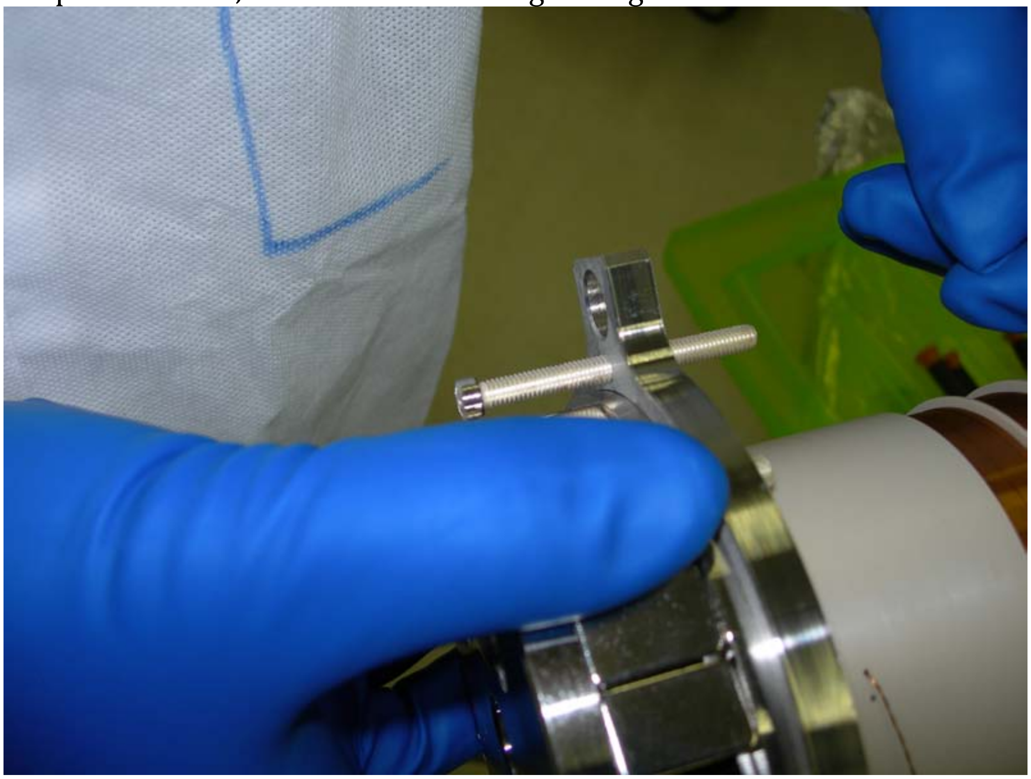

The LVDT secondary is presented below the filter

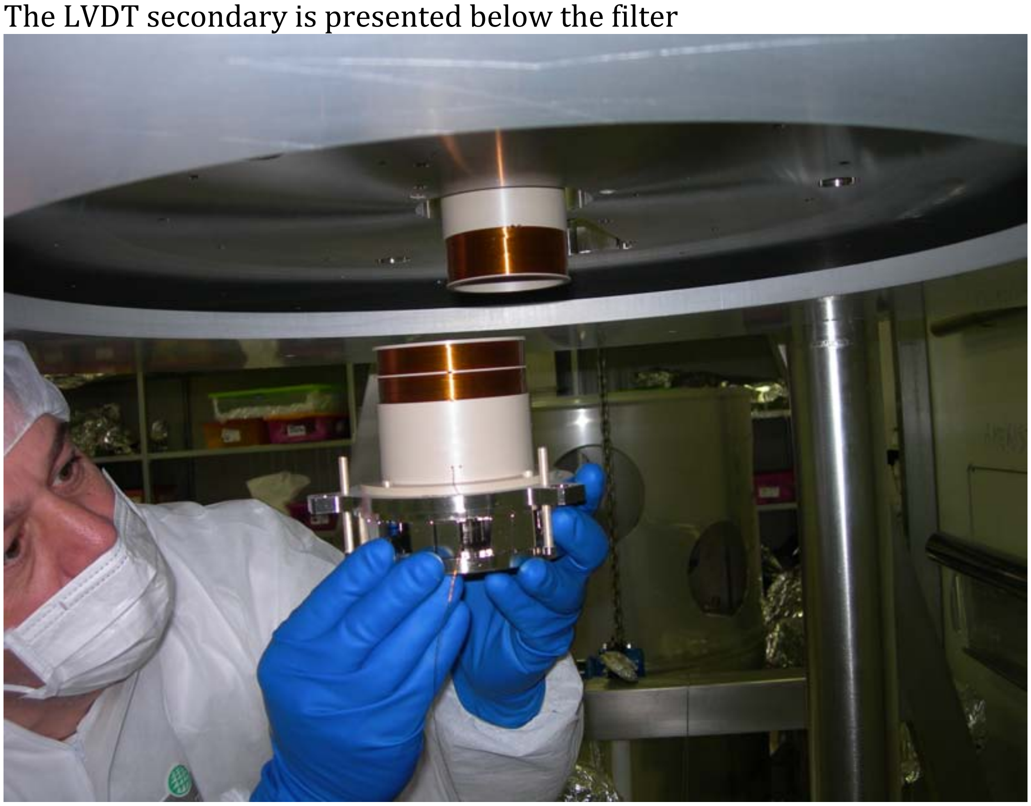

The three pulling screws are mounted

the three push and the three pull screws are used . . .

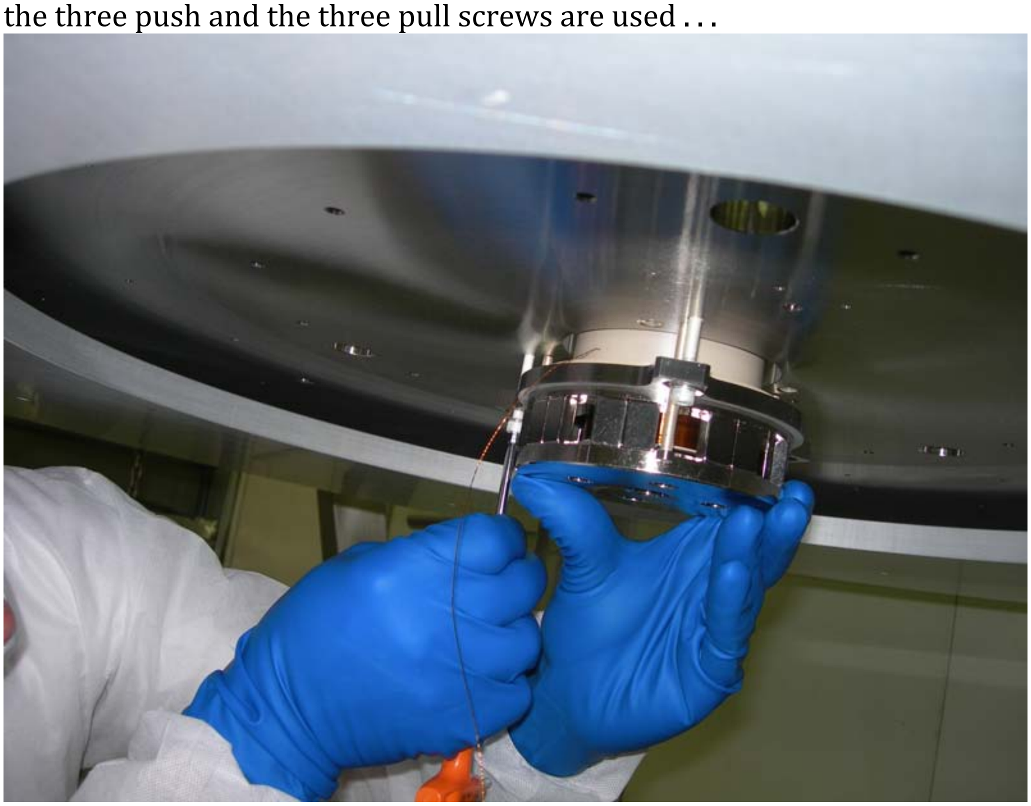

To align the top rim of the LVDT secondary to the groove in the LVDT primary. When this is achieved the LVDT primary is centered at the same height of the secondary middle point. Because the filter has been locked close to its working point, the LVDT will give ~0 V at the working point. Fine tuning will be needed after installation.

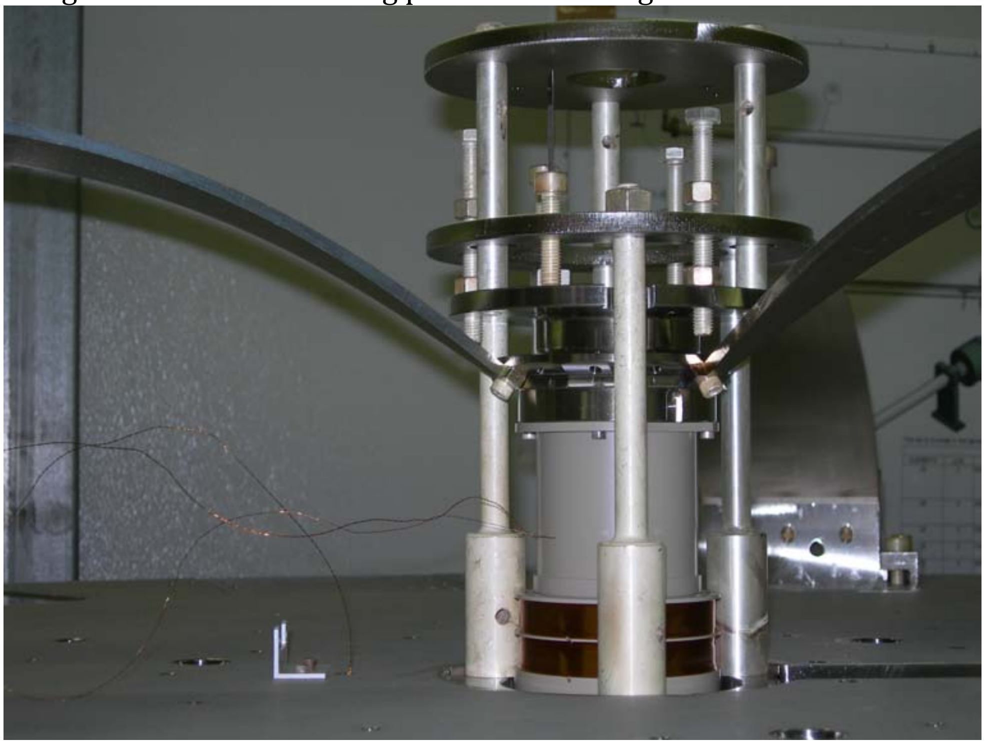

The push-pull screws are also used for the transversal centering of the secondary to the Keystone, which for the initial tuning is made with a PEEK wedge gauge, against the M12 load threaded rod.

In the chain assembly the LVDT secondary will be aligned to the suspension wires using this custom tool.

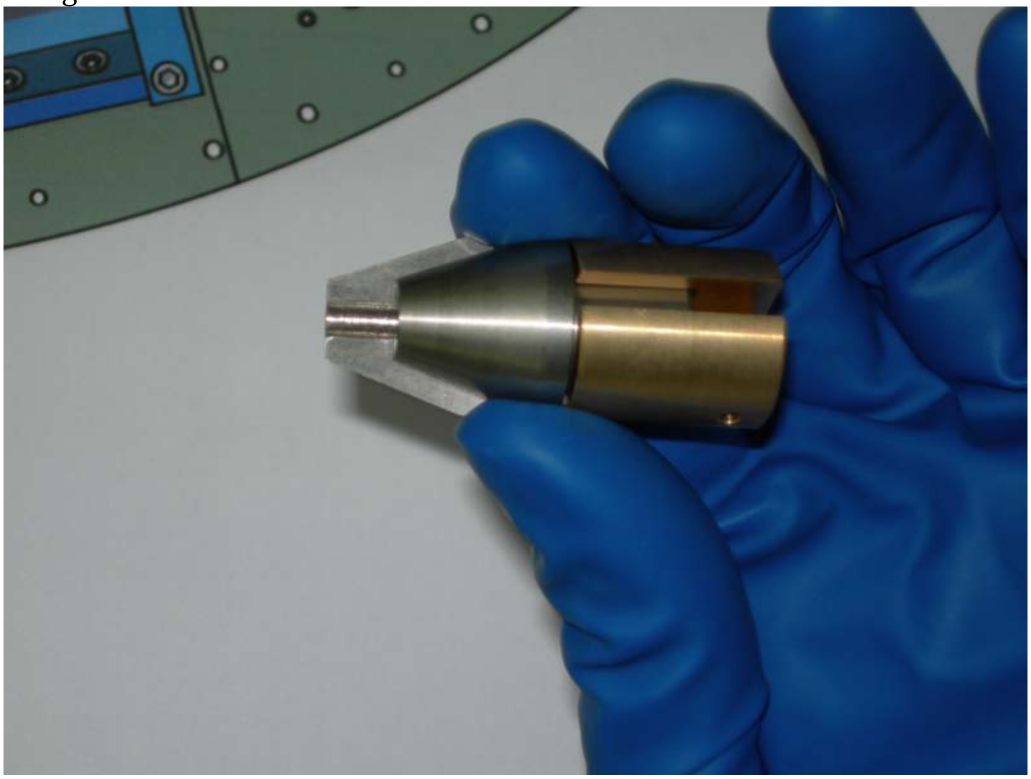

The wiring of the LVDT primary and secondary, and of the actuator coil are routed.

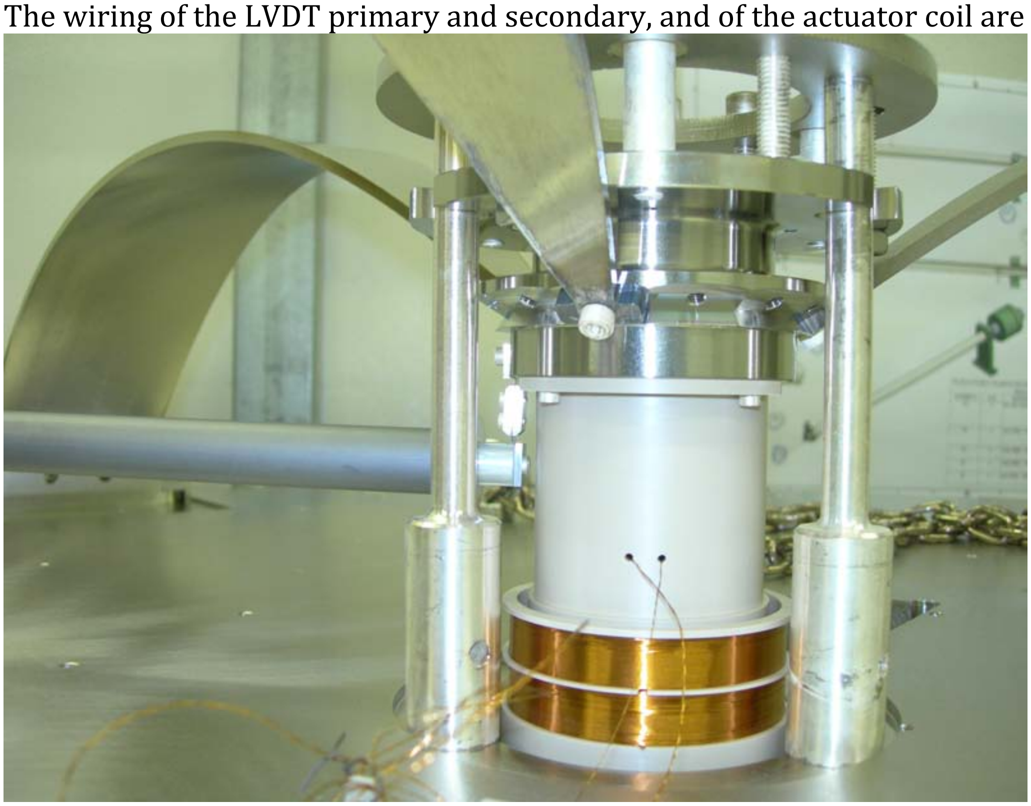

The connector flange is mounted (the connectors are not yet available).

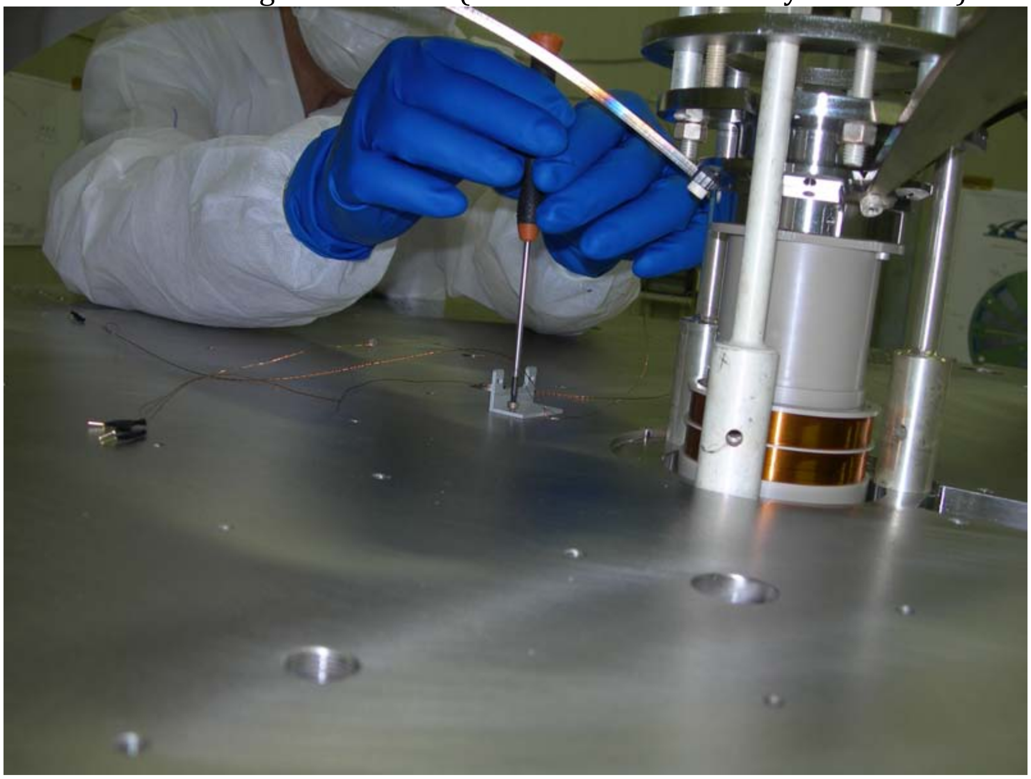

The cabling hexagon in mounted below the top filter

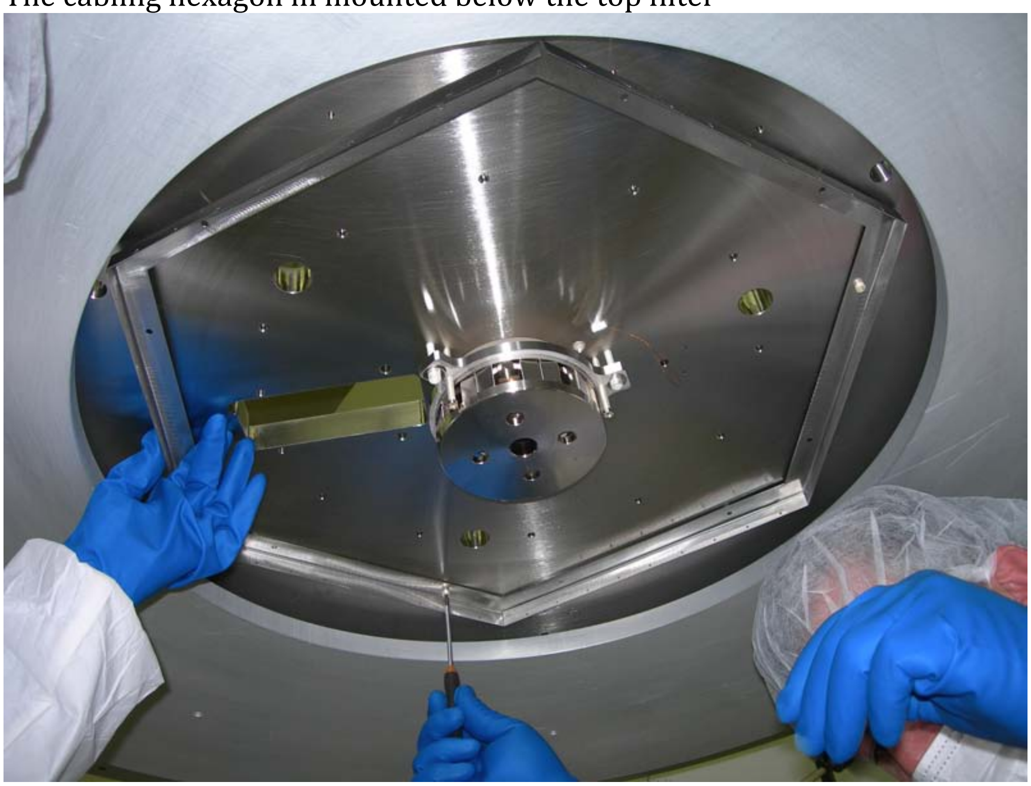

Measurement of the filter's Quality factor

Paolo Radaelli and Takanori Sekiguchi dedicated a week to the measurement of the resonant frequency of the filter as function of radial compression, and of quality factor as a function of resonant frequency.
For this task a Sting-ray USB oscilloscope is used, together with a NIKHEF type LVDT driver and a laptop computer.

The radial compression of the filter is changed by incremental steps, thus changing its resonant frequency. At each step the optimal working point of the filter is found, by changing load weights and, at low frequency, by help of the filter hysteresis (see separate report by Paolo and Takanori). Finally the filter oscillation is excited and recorded to study the filter's behavior.

The usual Square root behavior of the frequency versus radial compression is found.

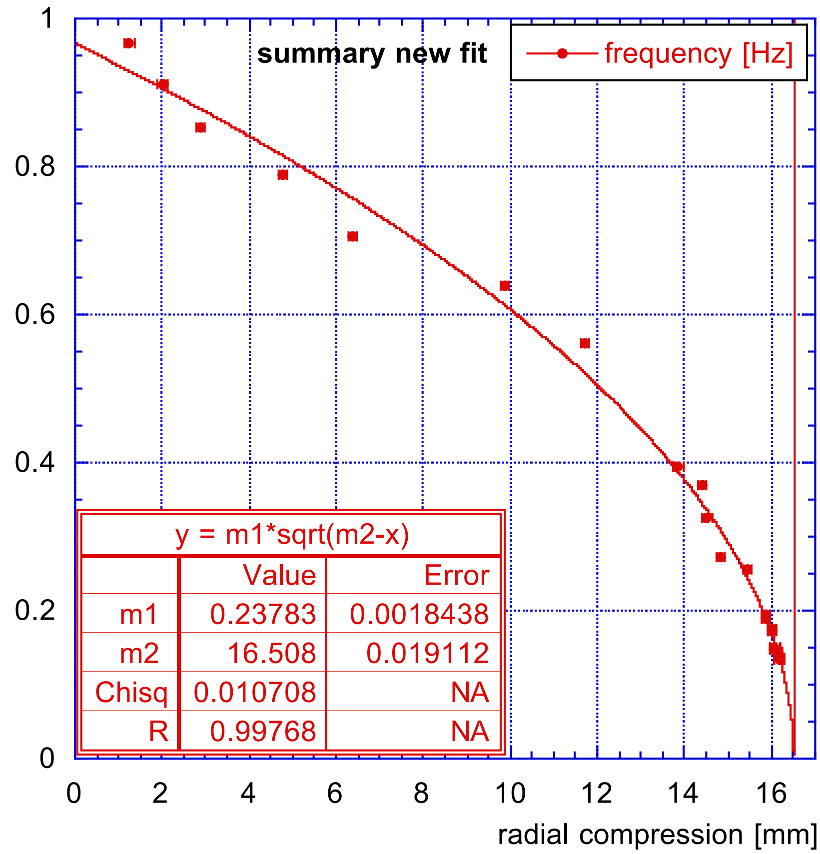

The oscillation quality factor of the filter is found to change over a very wide range, as already found in R. DeSalvo, A. DiCintio and M. Lundin, Eur. Phys. J. Plus (2011) 126: 75

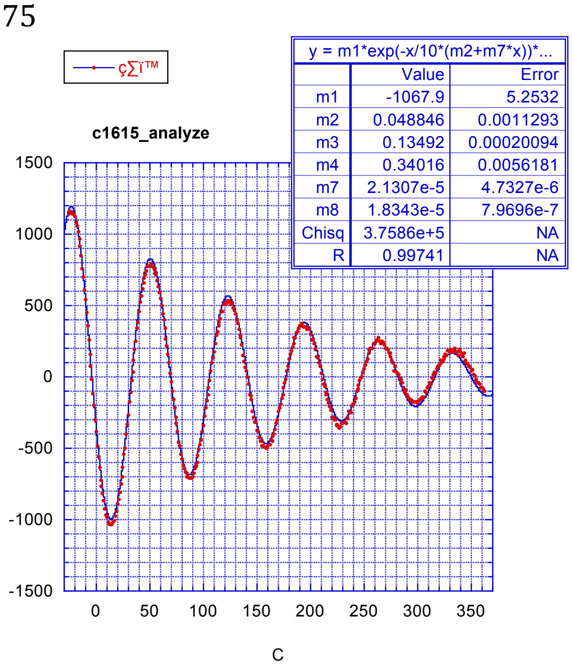

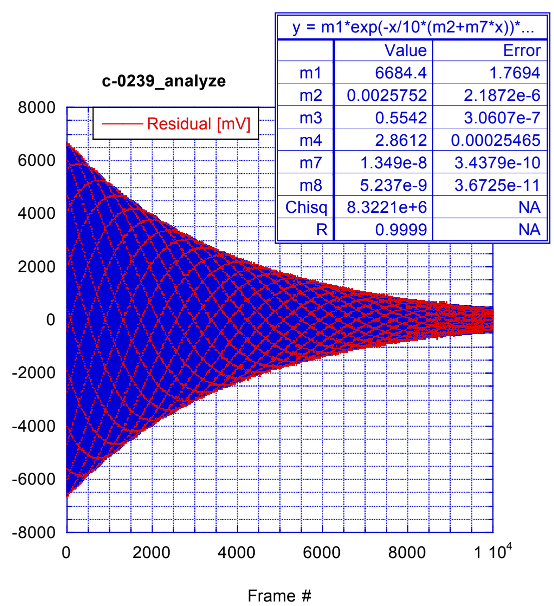

To analyze the data, the oscillation signal stream is de-trended by subtracting the average over the N points along an oscillation to eliminate any working point drift that may affect the result of a decay fit.

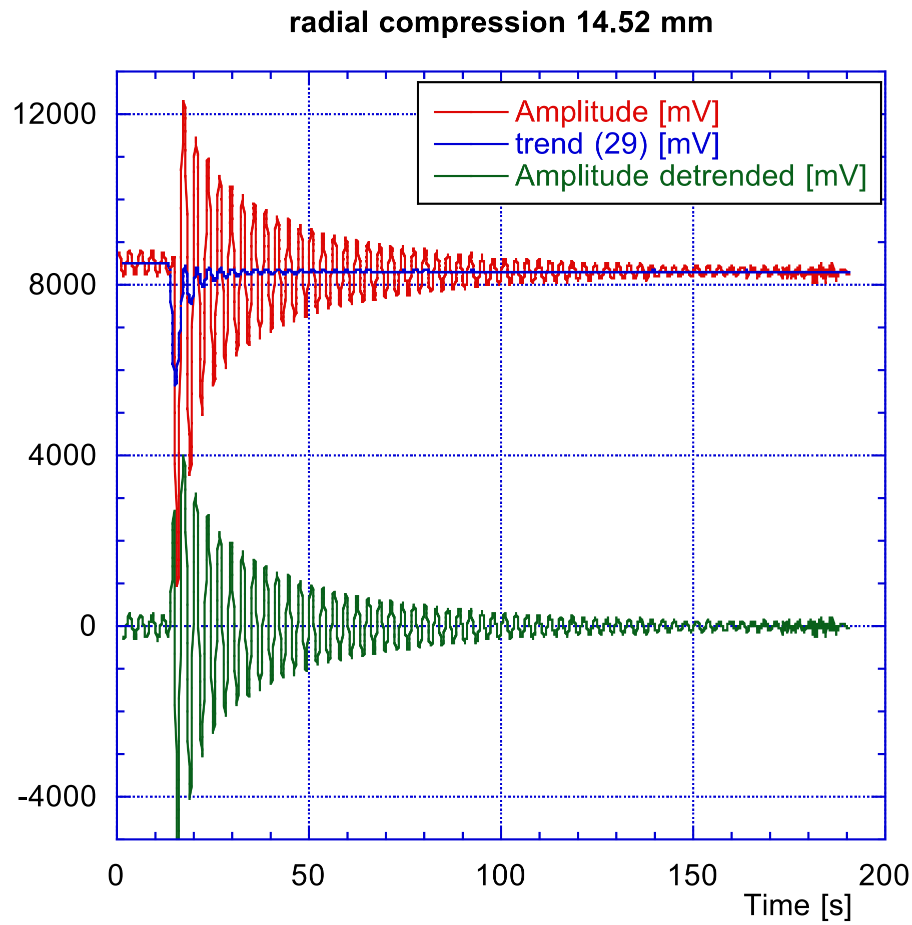

Then the absolute value of the de-trended amplitude signal is then considered to evaluate the oscillation decay lifetime. It is further averaged over the N points along an oscillation to retain only the decay trend, and filter out the oscillation.

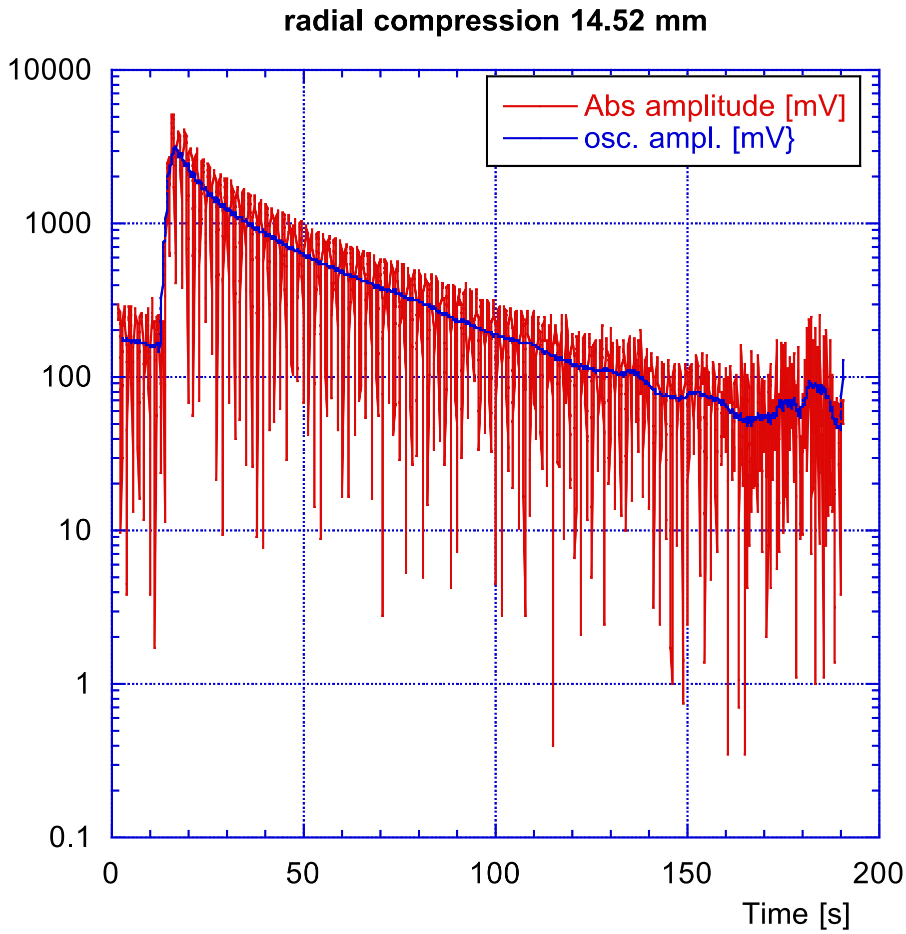

Finally the thus filtered data is fitted with an exponential decay, plus a noise level. The noise level is added either linearly or in quadrature to the decay. Both cases yield similar results. In the log plot it is clearly visible how, below amplitude ~ 100 mV (~40 μm) the machine shop ground noise start affecting the measurement.

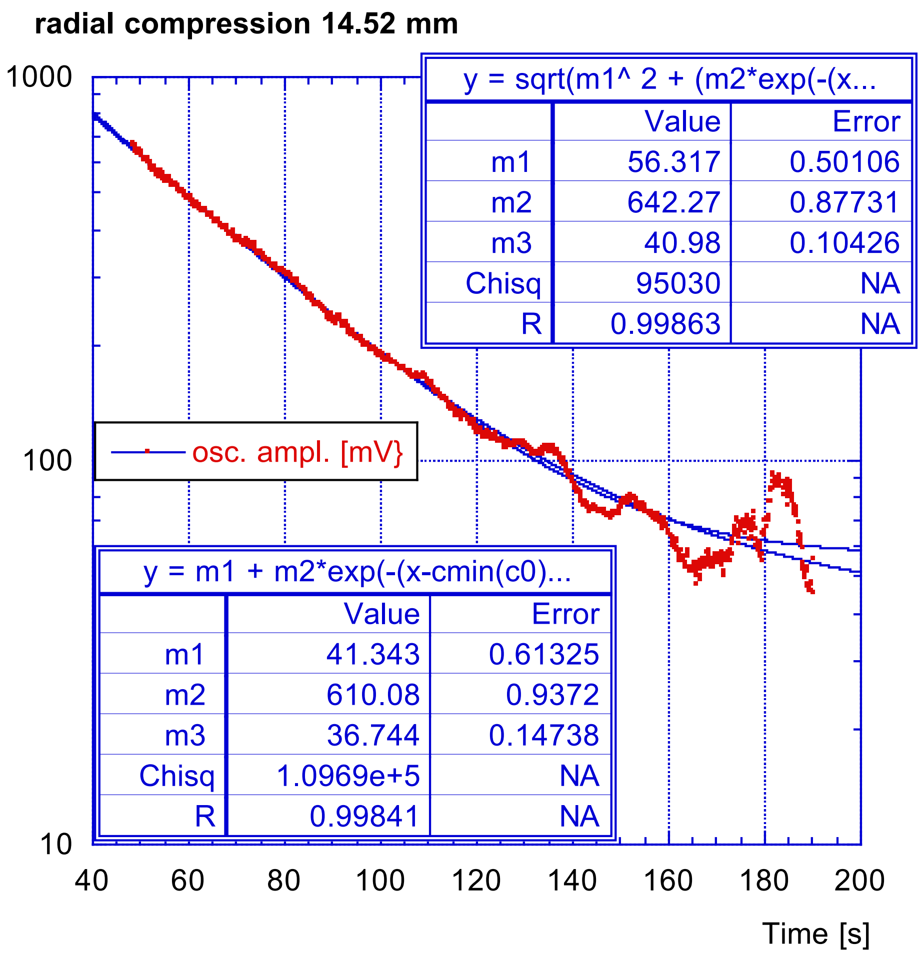

The quality factor versus frequency fits well with the quadratic plus exponential formula of R. DeSalvo, A. DiCintio and M. Lundin, Eur. Phys. J. Plus (2011) 126: 75, figure 30.

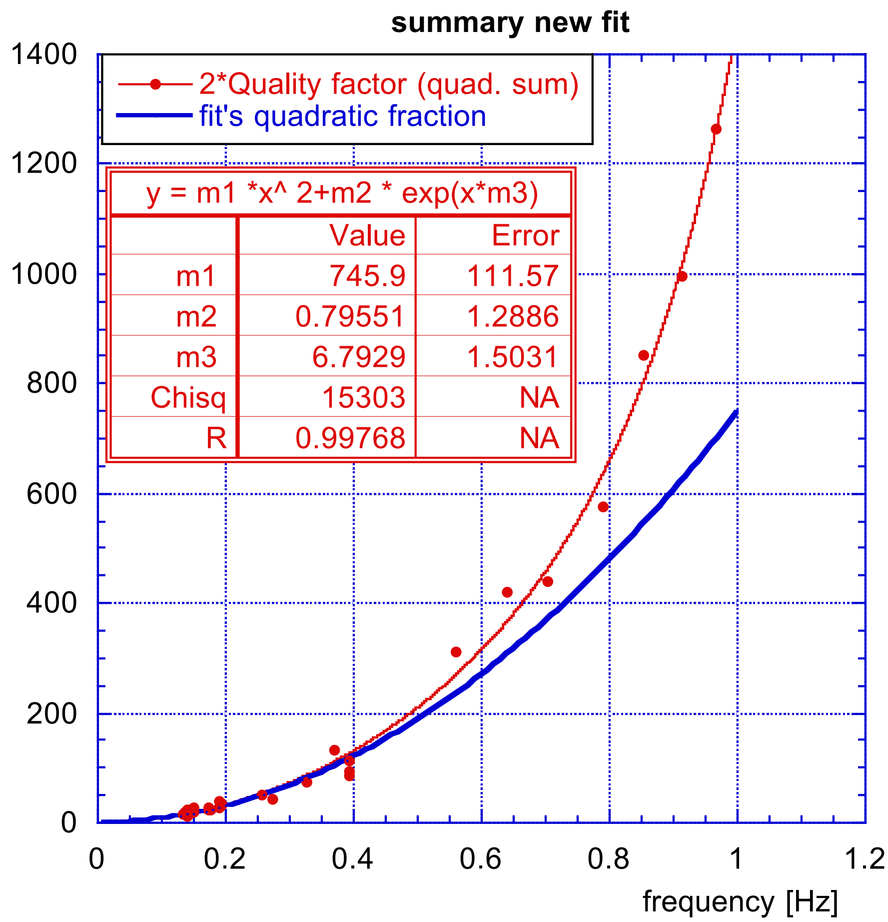

Comparing with the GAS spring tested in R. DeSalvo, et al., figure 30, the quality factors are higher, while the exponential departure point from the quadratic curve happens at 0.4 Hz instead of 0.2 Hz

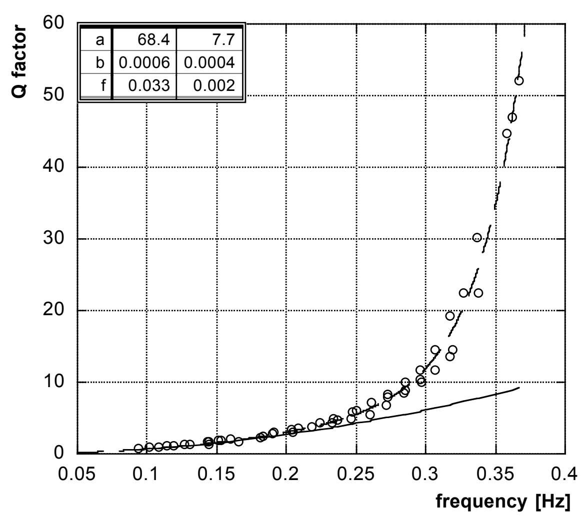

Conversely if a power fit is applied, it requires a power coefficient 2.8±0.1, very far from the quadratic term expected from purely hysteretic dissipation, and fits poorly the low frequency region (see lower insert)

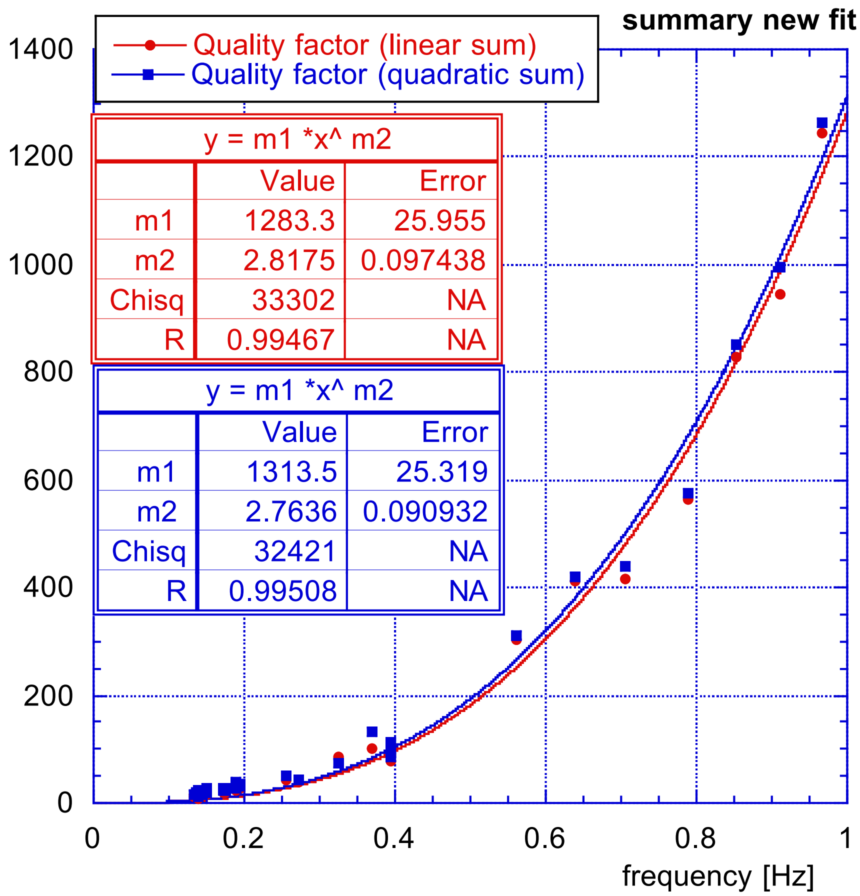

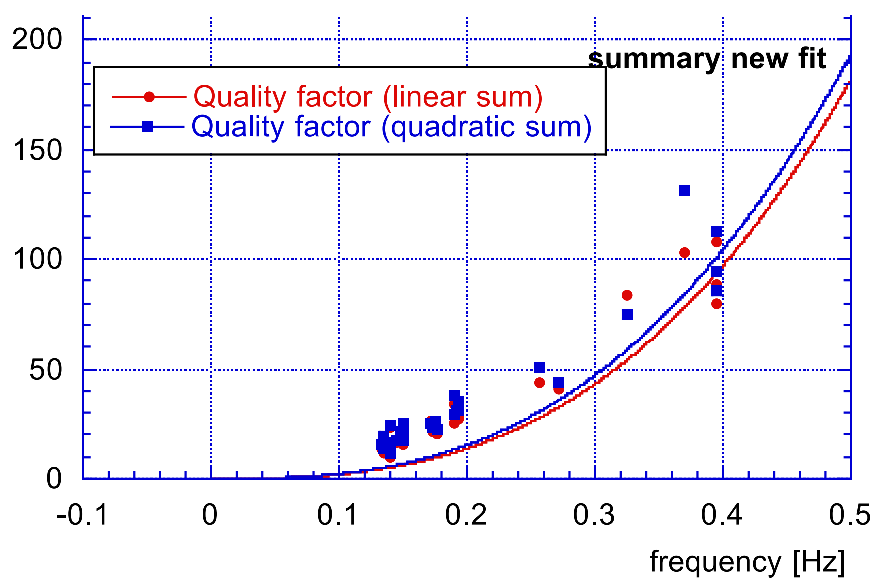

Assembly of the magic wands

The filter, as built has a maximum attenuation factor of 1000, due to the Center Of Percussion effect of the distributed mass of its blades. The performance can be increased to 10,000 or 30,000 by the addition of the magic wands in parallel to the blades. The magic wands are counterweighted rods bolted to the filter base plate and hinged to the filter keystone.

The first step of the magic wand assembly is to mount the counterweight threaded insert on the silicon carbide shaft. The hinged feet are prepared as well.

Then the shaft is inserted in the hinged foot, and locked, and the hinged cap is mounted at the tip of the shaft.

Finally the counterweight, formed by two cylinders, is screwed on the threaded insert.

The two counterweight cylinders are locked to each other

For assembly and transport the counterweights are mounted all the way in. In this configuration the magic wand is neutral and would have no effect. When installed, the counterweights will be moved backward by a pre-determined amount to generate the percussion point cancellation effect.

One magic wand for every three blades is foreseen.
The wand is brought to the filter.

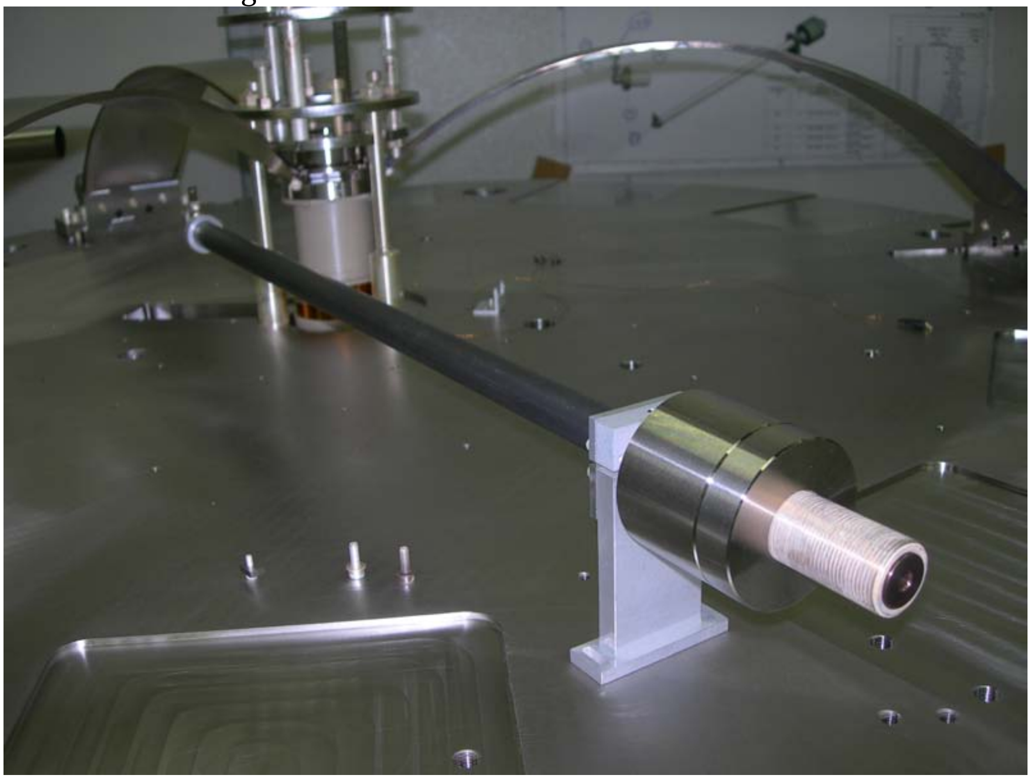

The tip of the wand is attached to the keystone.

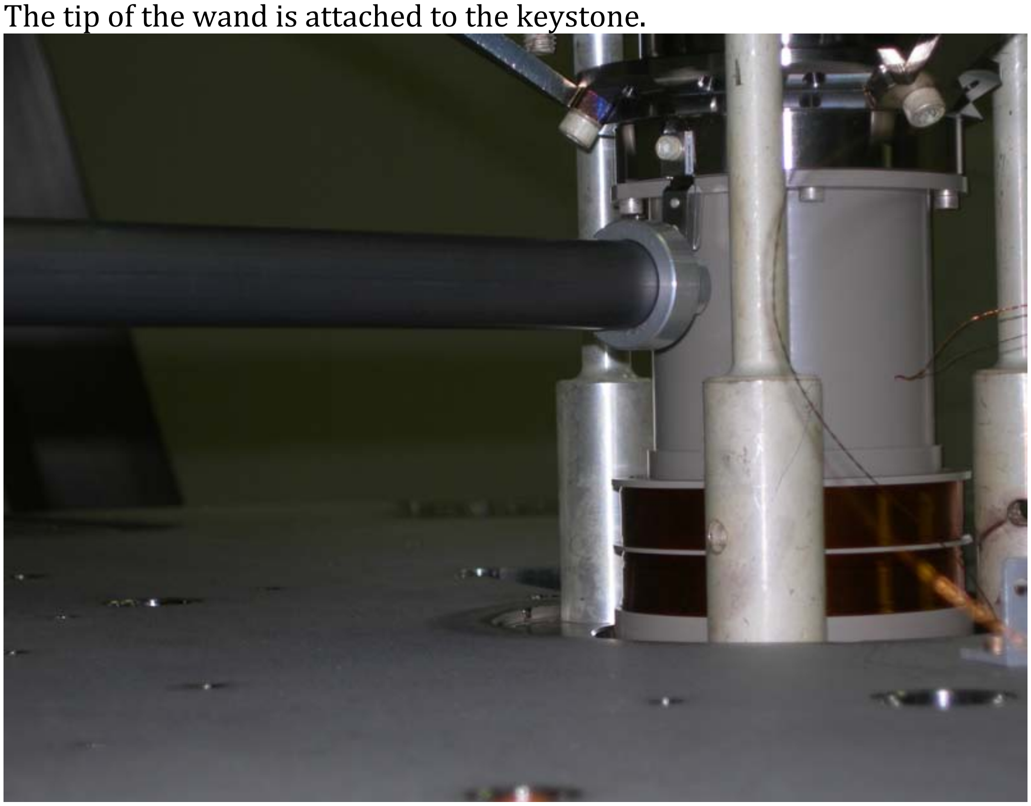

The magic wand foot is bolted to the filter's base plate.

Before locking the wand's foot to the base plate, the alignment of the tip hinge must be checked for verticality.

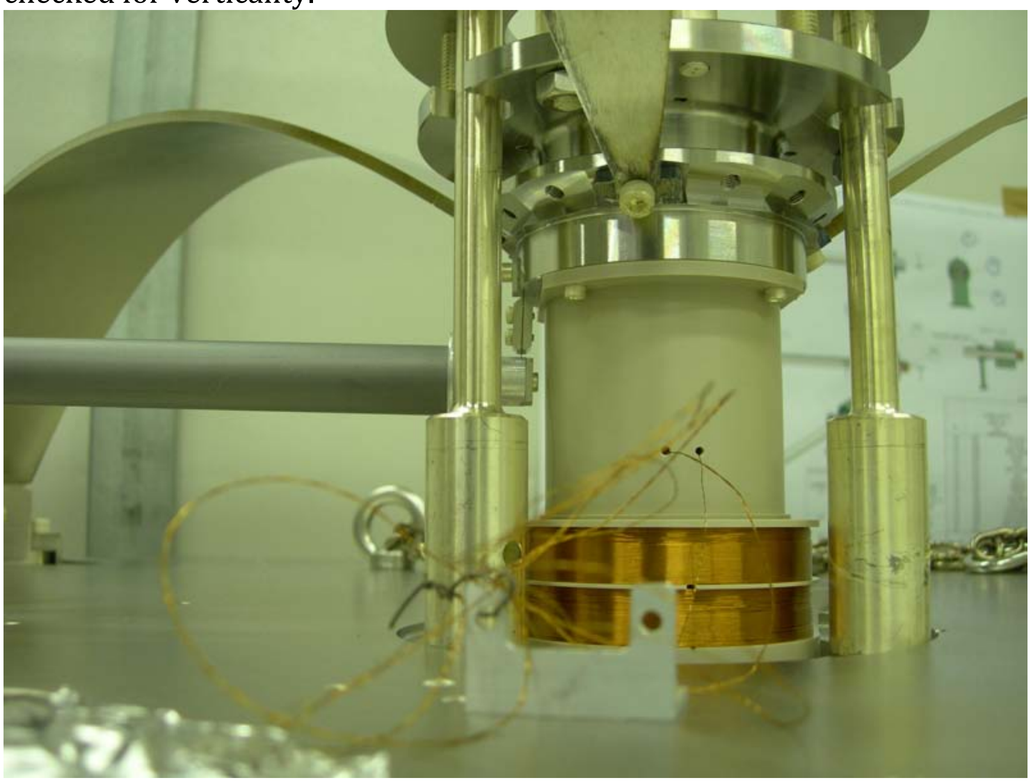

The magic wand is ready. The pre-isolator filter is ready for shipment, with the exception of the magnetic dampers and rotational mechanism, which are packed separately.

Chapter Moving and packaging

The finished pre-isolator filter is lifted and placed on its transport cart, and moved from the clean room to the pre-room. Three shipping feet are mounted on the base plate.

In order to keep the filter clean, it is not lifted directly by the crane, which may drip dirt. Instead the Oven cap is used as an intermediate dust and grease shield.

The filter is carried close to the base of the shipping crate. The shipping crate base is designed for fork lift use. A black water barrier sheet is placed on it. Three stainless steel stress relieve disks are placed on top, in the precise position where the shipping feet must be. Holes are drilled through the shipping base to receive the threaded rods protruding from the feet..

The filter is wrapped in UHV compatible aluminum sheet

The wrapped filter is lowered on the base.

After tightly bolting the feet on the base the first filter is ready for shipment

It is foreseen to ship two filters per box as illustrated below.

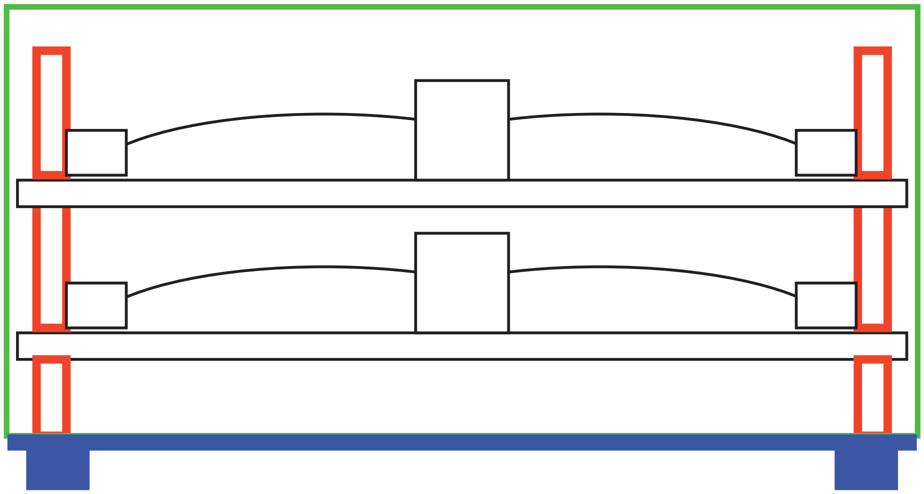

When a second filter is ready it is moved in, wrapped in aluminum foil and lowered on the waiting spacers of the lower filter in the crate.

The second filter is bolted to the spacer

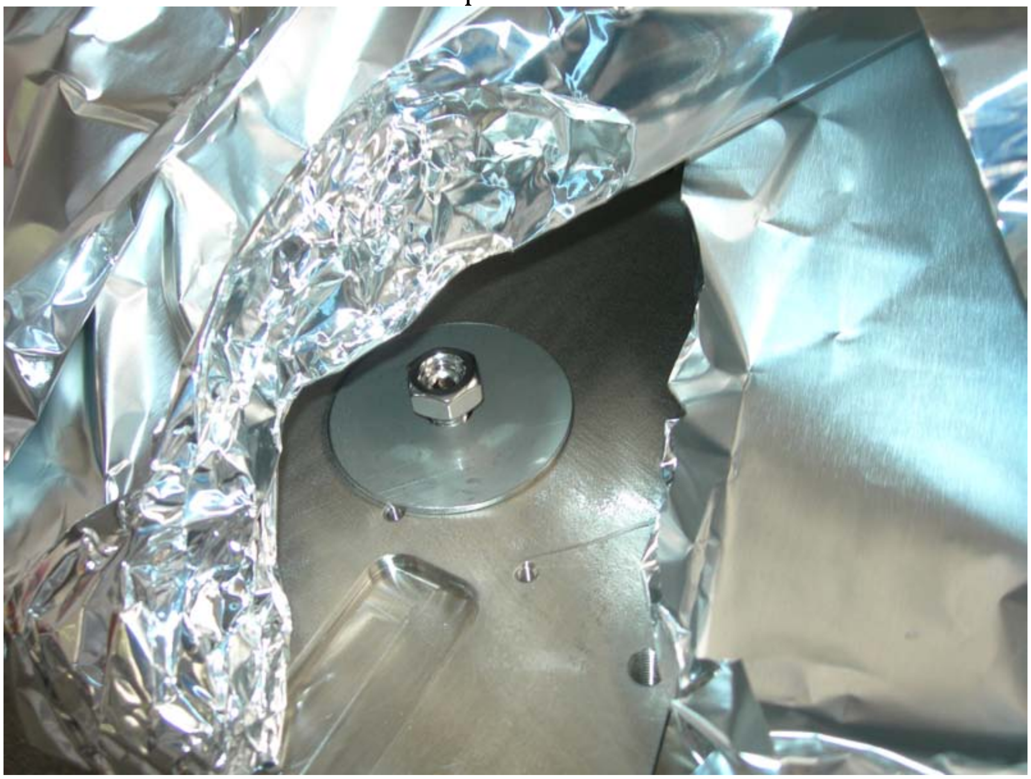

and tightly locked for overseas shipment.

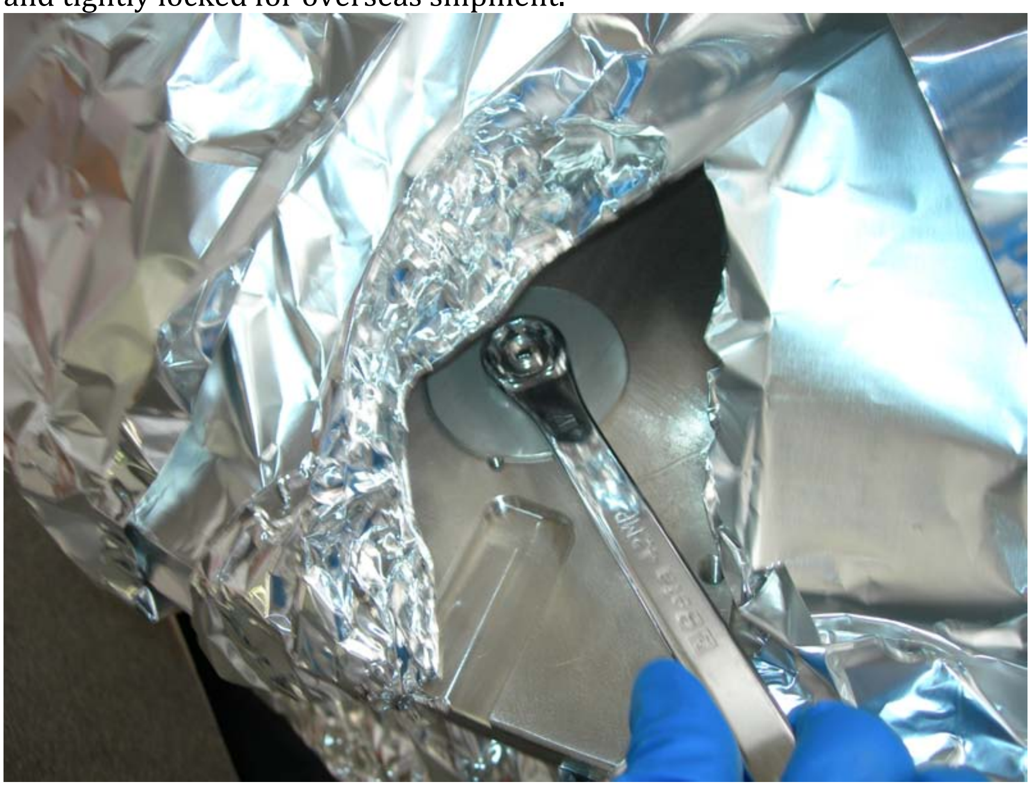

Finally the capping part of the water barrier bag is lowered over the filter, water absorbing bags are placed below the bottom filter, and the cap is hermetically welded to the base sheet. Before welding of the final section, the bag is vacuumed to remove as much air as possible in the water proof bag, to allow for expansion of the bag, for air freight shipment.

At the end the side panels of the shipping crate are screwed on the sides of the base, then two spreader beams, and finally the cover of the crate is screwed in place. Two pre-isolator filters per box are ready for shipment. Three crates for a total of six pre-isolator filters will be shipped in 2013.
At receiving, the top cover must be unscrewed first, and removed, then the two spreader beams unscrewed and removed, then the side panels.

Rotation mechanism

Both the rotational mechanism and the motorized spring for vertical working point adjustment could not be installed because the UHV compatible motors will be procured separately.

The rotation mechanism mounts above the blade's keystone. A long-thread nut is bolted on a castle structure attached on the keystone top surface of the keystone.
A DLC lubricated threaded-shaft stepper motor mounts into long thread brass nut. A thin U-blade impedes the rotation of the motor, while it allows its longitudinal motion. The tip of the motor shaft pushes on a flag, mounted on a cup that on the outer diameter sits on a bearing seated on the keystone, and on the center has the key-hole receptacle for the main suspension wire.

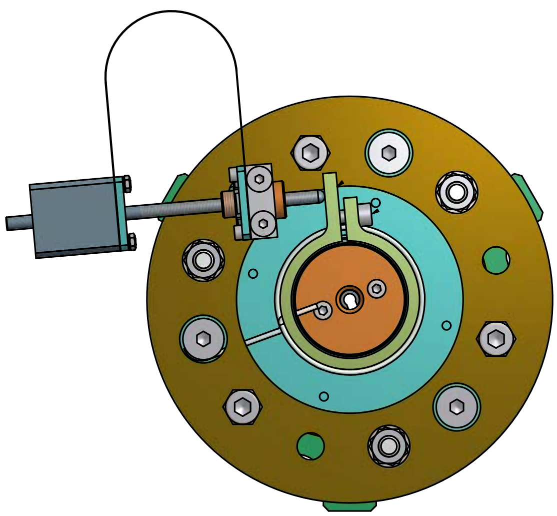

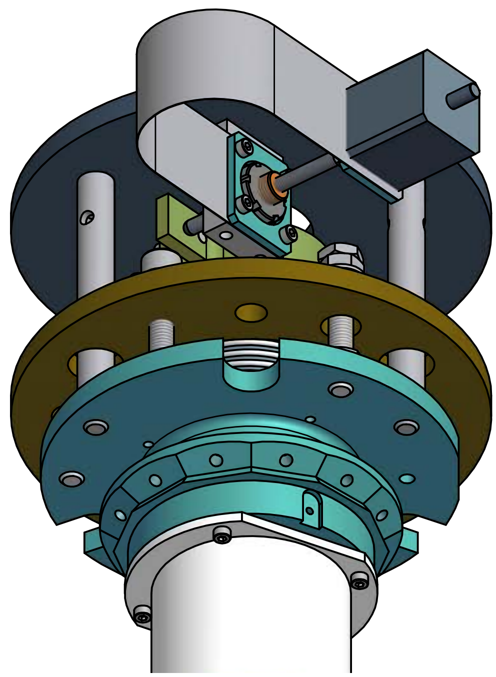

The rotation mechanism rolls on a semi standard shaft bearing, with high quality Sapphire balls to prevent cold welding in vacuum.
Standard bearings were procured, the ball cages were emptied of the existing metal balls, their racetracks and ball cages and the balls were ultrasound washed and baked in air at 200°C.
It was found impossible to insert the aluminum oxide balls in the ball cage without damaging them when balls and racetrack were UHV clean. To solve the problem we procured some hydro-soluble oil, and re-wetted the balls and ball cage. After that the balls could be re-inserted easily. Finally we vigorously washed the re-furbished ball cages in hot ultra-sound bath with degreasing detergent for a few hours, rinsed them in water, rinsed in de-ionized water, and finally rinsed in analysis grade alcohol to remove the water. A final bake finished the preparation process.

After that the bearings were reassembled and worked properly, ready to be mounted on the rotation cup.

The rotation cup has the keyhole receptacle for the main suspension wire, a number of holes for the assembly of the torque restoring spring, and a flag, mounted on the cap, that will be acted upon by the stepper motor to generate the rotation.

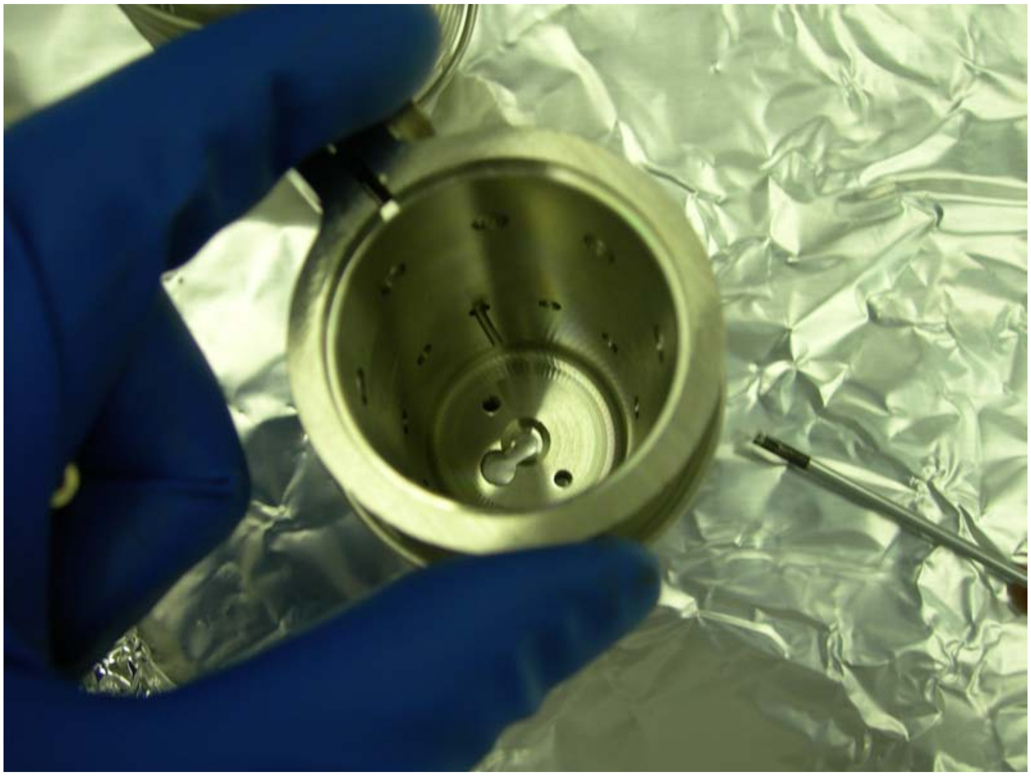

During installation of the chain, the suspension wire may be lifted and disengaged from its seating. To avoid the suspension wire to move sideway in the key-hole, and fully disconnect, or seat crookedly and be damages, a safety ring is foreseen.

The safety ring bolts at the bottom of the cup, after the suspension wire is in place. It will allow the vertical motion and rotation of the wire without allowing it to misalign laterally. The flag cap and its radial screw locking mechanism is visible as well

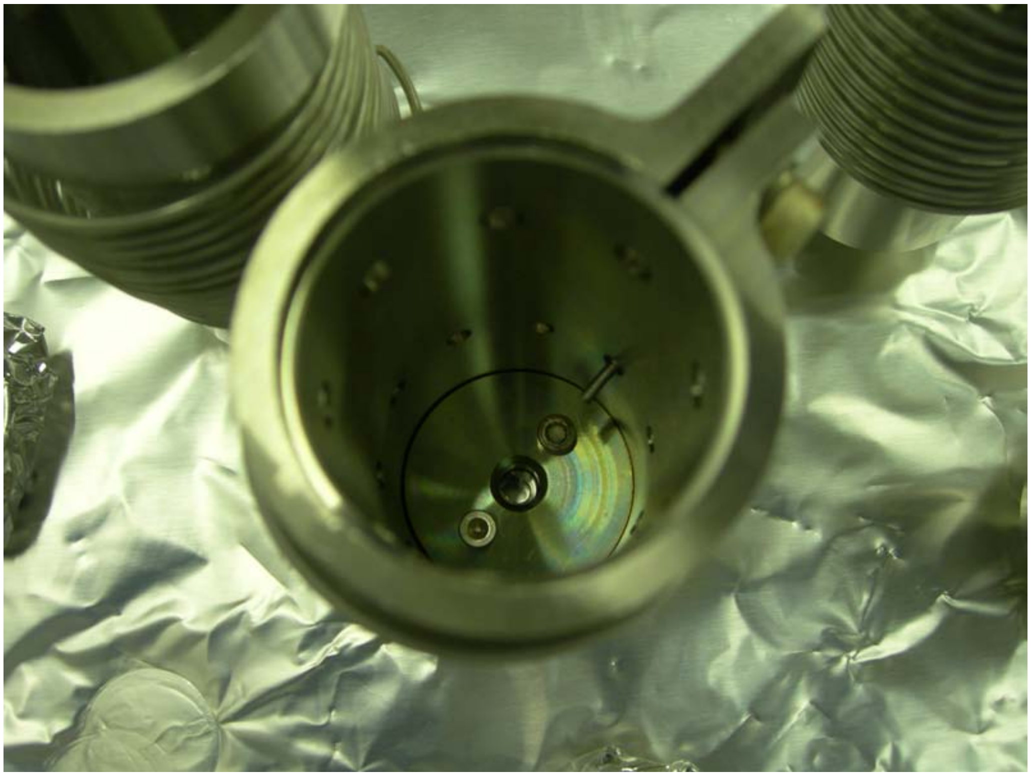

The flag cap can be easily oriented on the cap by means od two screwdrivers, one through holes designed for this purpose, and one in the locking mechanism slot.

The anti rotation blade, the nut stand and the brass nut are mounted together. The flange mounting on the stepper motor is temporarily attached.

The mounting of the nut and the anti rotational blade are tested on the filter, then disassembled.

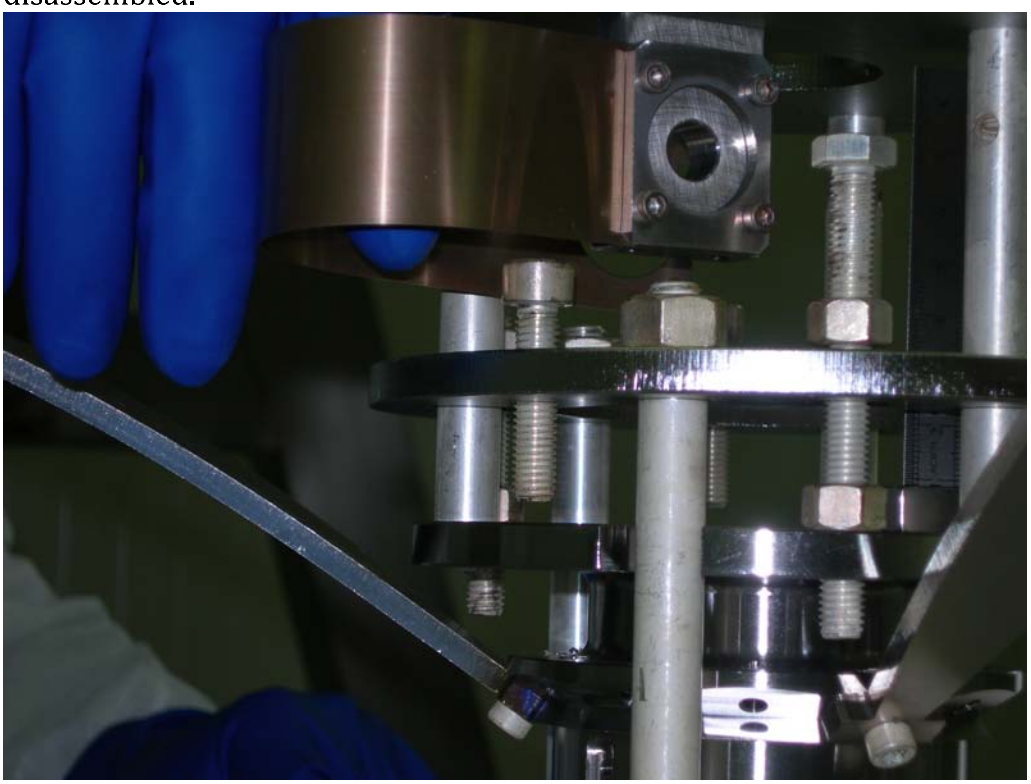

The parts of the rotational mechanism are then ready for packaging and shipment

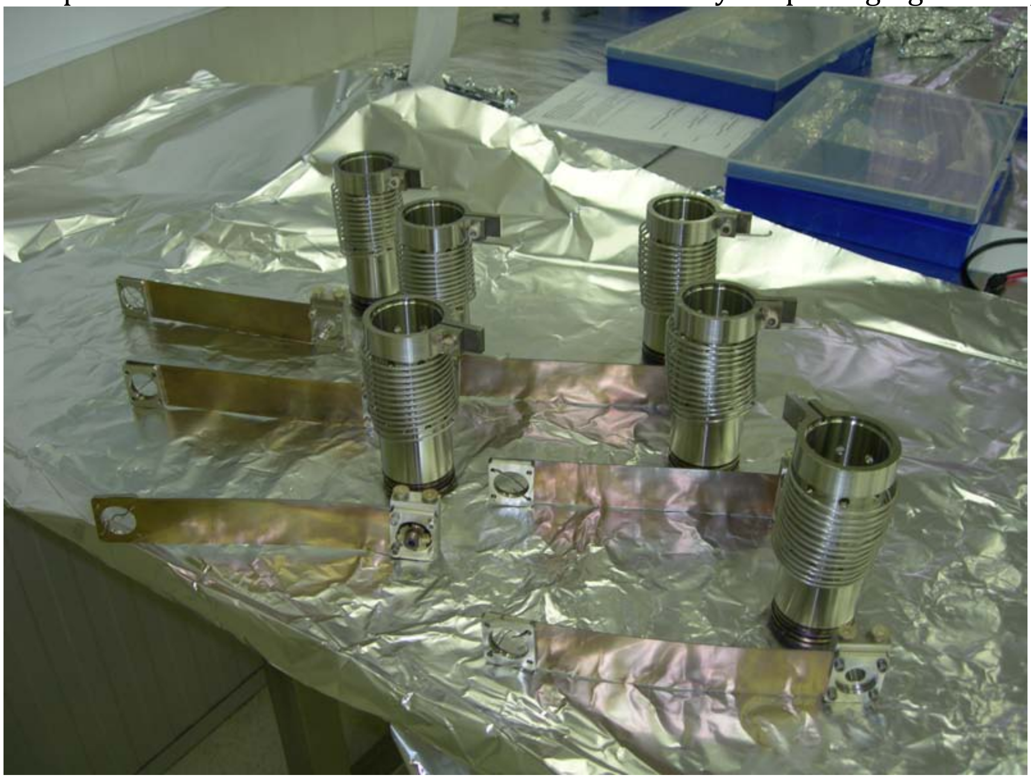

Vertical motorized spring

The vertical motorized spring tunes the working point of the keystone. It uses the same motor of the rotational mechanism. The motor is mounted on a flange, mounting on the filter bottom flange. The end of the spring bolts to the side of the filter's key-stone.

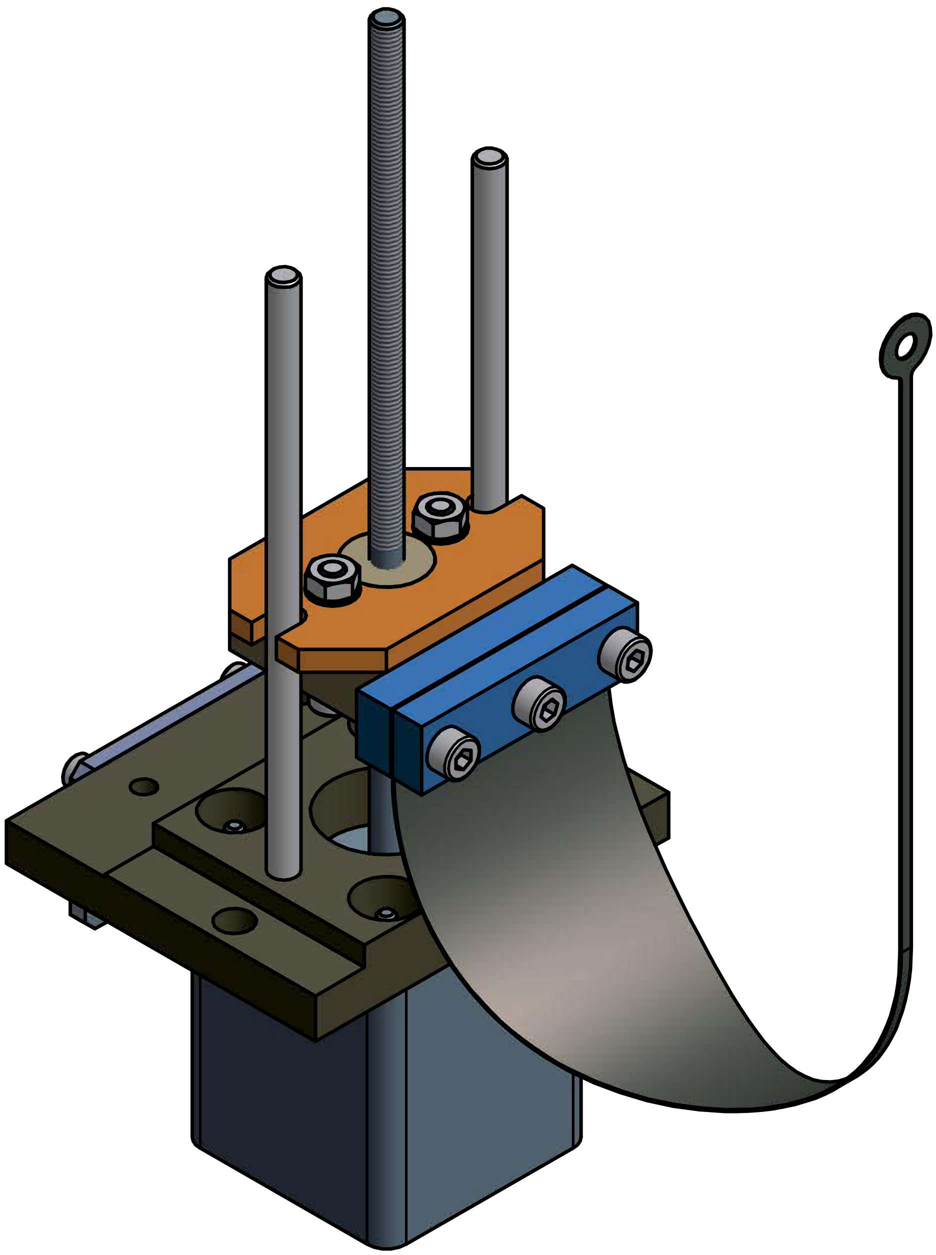

The peek nuts are mounted on the anti-rotation flange

Then they are mounted to the blades

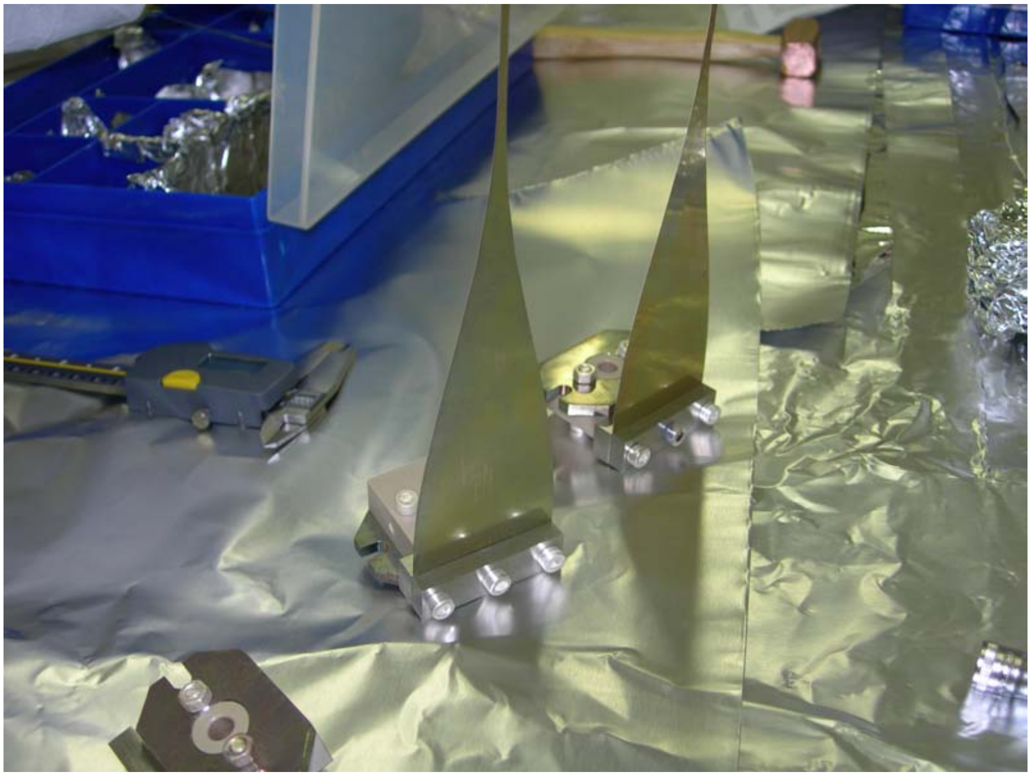

The anti-rotational rod is forced in the flange supporting the motor.
Two anti-rotational rods are foreseen, but only one is mounted, because it may be sufficient and two rods may render the movement harder. The second rod is packaged together.

The flange supporting the motor is test mounted below the filter base plate. The fitting was not perfect and correction shims were manufactured and packaged with the flange.

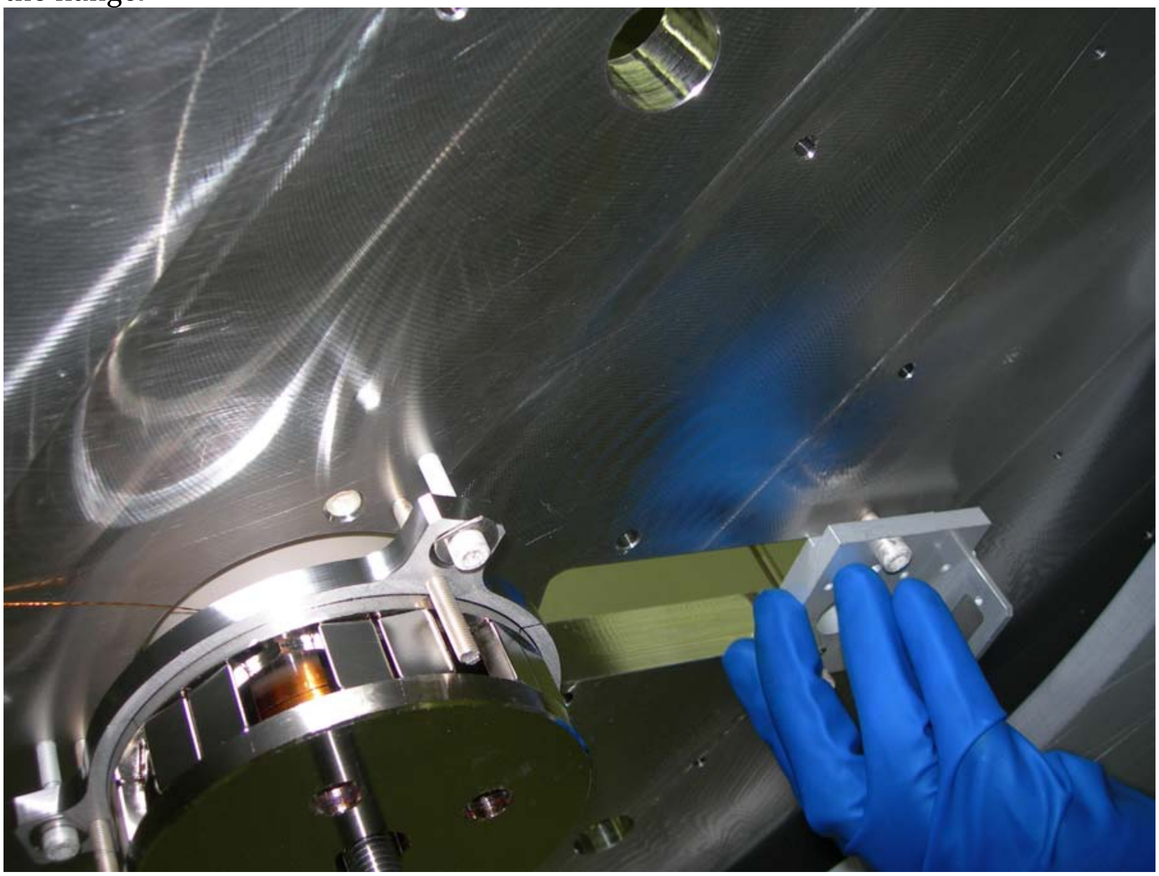

Magnetic dampers

The magnetic dampers are formed by a soft iron ring, suspended from the bottom of the top filter and supporting a matrix of 12x12x12 mm magnets, and a OHFC copper ring mounted on the roof of filter 1 of the attenuation chain. The copper ring is built in three 120^{o} sections joined by bolted plates.

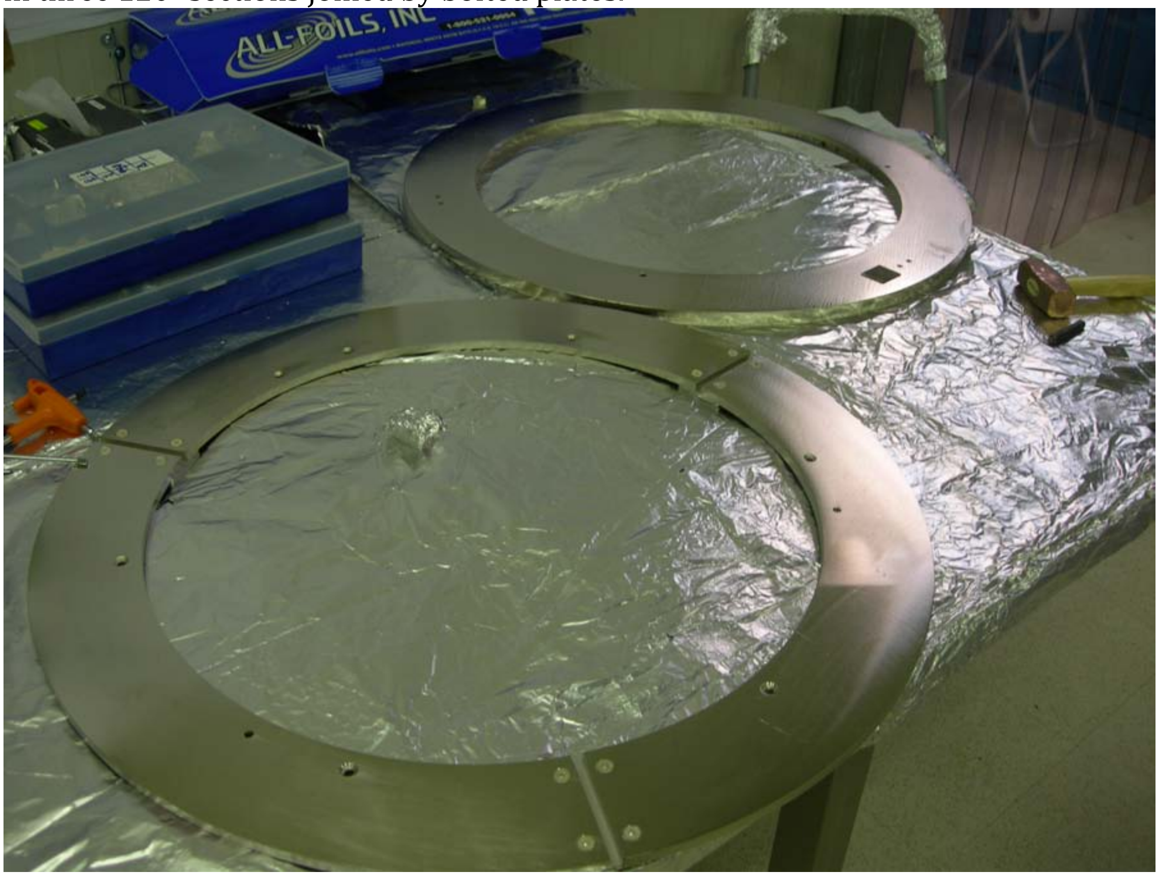

The suspension wire clamps are mounted on the disks while the suspension wire nuts mounting on the top filter are packed separately. The suspension wires are shipped separately.

Each iron and copper ring pair are temporarily bolted together and aluminum packed for shipping.

All parts are crated inside a water proof bag.

Rings, rotational mechanism, vertical spring mechanism wire suspension nuts and all other small parts are packed together

Water absorbing packs are added before welding the water barrier bag closed

All crates are shipped to Japan